

#### CHAPTER IV

### S T R U C T U R A L   G E O L O G Y

#### STRUCTURAL PATTERN

The structural geology of the Almora area at first sight appears to be simple, but its detailed structural investigation has revealed an interesting and somewhat complicated history.

The study area is situated almost on the hinge of the Almora nappe synform and its rocks contain structural evidences of an interesting tectonic history, comprising a series of deformational episodes.

The author has been able to decipher the structural complexities of the area with the help of (i) a systematic and detailed mapping of the lithological units and the various macroscopic and mesoscopic structures, (ii) a critical analysis of all the structural elements - both planar and linear, and (iii) structural patterns of the neighbouring areas of Ranikhet and Majkhali as worked out by the previous workers.

For the most part, the rocks in the area show a north dipping foliation. The main synformal fold axis is encountered in the north eastern part, where it is seen passing from the villages Dinapani and Kaparkhan. A small portion of the northern limb of the synform is recorded in the extreme NE corner of the area near the villages Sheora, Patiya and Kasaun. On this limb, the foliation dips due S.

Although the Dinapani-Kaparkhan synformal fold is the most striking structural feature of the area, there are ample evidences to suggest the existence of yet another fold episode, older to the folding of the Almora nappe. Numerous tight isoclinal (almost reclined) folds in quartzites indicate a very early folding episode, which took place prior to the formation of the synform.

This early isoclinal reclined folding has been ideally studied and described by Vashi (1966), Vashi and Merh (1965) and Desai (1968) in the neighbouring areas.

Before proceeding with a systematic description and analysis of the structural elements of the area, the author has preferred to give below briefly and chronologically the main events of the area's structural history as worked out by him with the help of his own study and the available data of previous workers:

- (1) Deposition of sediments under geosynclinal conditions and their subsequent metamorphism under vertically directed load, giving rise to a bedding schistosity (S).
- (2) Folding of the metamorphosed sediments into a number of isoclinal reclined folds ( $F_1$ ); development of the axial-plane foliation ( $S_1$ ) and the related fold axis lineation ( $L_1$ ). Culmination of overfolding into Almora thrust and the formation of Almora nappe.
- (3) Folding of the Almora nappe into an E-W synform. This folding affected both Almora and Krol nappes, and resulted into the formation of the anticlines

- at Someswar in the north and Bhowali in the South. This folding gave rise to microfolds and crinkles in schists with an associated strain-slip cleavage ( $S_2$ ). The fold axes of these crinkles and puckers, and the intersection of  $S_1$ - $S_2$  characterise the related lineation ( $L_2$ ).
- (4) Superimposition of open N-S to NE-SW flexures ( $F_3$ ) on both the limbs of the synform. Fluctuations in the strike trend at most places and the development of a faint crinkling on the foliation and related puckers ( $L_3$ ), are attributed to this episode.

In deciphering the structural pattern of the area, the author has mainly relied on the trends of the foliation and its dips in the different parts. The maps (Figs. III.1, III.2 & IV.4) typically reveal existence of a number of synforms and antiforms, that developed during the second ( $F_2$ ) and third ( $F_3$ ) foldings. The geometric analysis of the linear and planar structures, related to the various fold episodes, has enabled the author to work out the details of the effects of successive episodes and their mutual interference.

In the following pages of this chapter, the author has given a detailed account of the various major and minor structures and also their critical analysis.

## MAJOR STRUCTURES

The structural pattern of the area comprises several macroscopic folds belonging to different tectonic episodes (Fig.IV.3). These folds have been classified and described as under:-

### Related to $F_1$ -

1. Several partly obliterated isoclinal (almost reclined) macroscopic structures exhibited by the shapes and trends of the quartzite outcrops in the central part of the area.

### Related to $F_2$ -

2. Dinapani-Kaparkhan Synform (in the NE)
3. Sual Antiform (Mid. E)
4. Guna Synform (in the SE)

### Related to $F_3$ -

5. Matela Antiform (in the W).

A brief account of the geometry of these folds is given below. The author would like to point out that the classification and geometrical identification of these folds is based on the results of the structural analysis which are discussed in subsequent pages.

### Early isoclinal folds ( $F_1$ )

These folds are conspicuous on the map, and are typically recognised by shapes of the numerous quartzite layers occurring in the schists. The entire zone of alternating quartzite-schist sequence represents numerous folded reclined structures whose axes plunge due N. The foliation of the schists typically shows axial-plane relationship with these quartzite folds.

### Dinapani-Kaparkhan synform ( $F_2$ )

This structure encountered in the NE represents the actual hinge of the Almora nappe synform. The axial trace of the synform that runs ENE-WSW, is almost sub-horizontal or plunges very gently to the ENE. Both the limbs of this synform, are considerably affected by the late  $F_3$  flexures, and as a result of this superimposition, the entire fold has become somewhat distorted.

### Sual antiform ( $F_2$ )

In the mid-eastern part of the area, this fold is recognised as yet another structure related to  $F_2$ , superimposed on the early  $S_1$  foliation. It is a fairly open yet quite sharp antiform, two limbs of which dip due NE and SE. The outcrop pattern ideally shows the interference

of  $F_1$  with  $F_2$ , and the  $F_1$  folds in quartzites are seen to be refolded on an E-W axial-plane. The fold axis shows a gentle plunge due E.

Guna synform ( $F_2$ )

This synform lies to the south of the above antiform, of which it forms a complementary fold. It has almost the same geometry as the Sual antiform. The synformal shape is impressed on the schistosity only, and no early macroscopic  $F_1$  folds are seen involved in this folding.

Matela antiform ( $F_3$ )

This rather big antiformal structure is seen in the western half of the study area, and is related to the last fold episode  $F_3$ . It is a fairly open structure arching up the schistosity along NNE-SSW axial-plane. The quartzites and schists - both are involved in the folding, as a result of which the foliation in the W and NW dips between NW and NNW, and comprise western limb of the antiform, the eastern limb dipping due NE. The axis of this antiformal structure has been found to dip gently due NNE. It is significant that the Kosi river flows along the strike of the axial surface of this fold.

## MINOR STRUCTURES

The various minor structures both planar and linear recorded and analysed by the author could be assigned to the one or the other major structures described above. Thus, it is so obvious that the structural elements preserved in the rocks of the Almora area, developed during the successive fold episodes  $F_1$ ,  $F_2$  and  $F_3$ . Before proceeding with a systematic analysis of the structural data, the author has given a short account and description of the planar and linear structures mapped (Figs.III.2, IV.1 & IV.3).

### Planar structures

1. Bedding and bedding schistosity
2. Axial-plane cleavage (main schistosity)
3. Crenulation cleavage

#### 1. Bedding and bedding schistosity

The traces of original sedimentary bedding, though very much obscured and obliterated, have been frequently recorded in the form of surfaces of folded quartzites. At some places, the lithological boundaries between mica schists and quartzites also indicate the bedding. The schistosity developed parallel to the stratification may be due to load. This bedding schistosity (S) was tightly



folded at the time of the isoclinal folding ( $F_1$ ), and this phenomenon is recognised occasionally on mesoscopic and microscopic scales. The tight folding of the bedding schistosity (S) developed into the main axial-plane schistosity ( $S_1$ ).

## 2. Axial-plane cleavage (schistosity)

This comprises the main schistosity ( $S_1$ ) in the area. The mica-schists and gneisses show a well developed foliation which shows axial-plane relationship with the reclined quartzite structures. Obviously this foliation was produced at the time of the large scale reclined ( $F_1$ ) folding of the area. A careful scrutiny of this foliation ( $S_1$ ) has revealed that it has evolved by the tight microfolding of the early foliation (S). Wherever the folds are recognisable,  $S_1$  is found to be parallel to the axial-plane intersecting 'S' at high angles at the fold closures.

## 3. Crenulation cleavage

Due to the microfolding of schistosity ( $S_1$ ) during the synformal folding ( $F_2$ ) of the Almora Nappe (Plate IV.1), a fine crenulation with associated cleavage ( $S_2$ ) has developed. The cleavage is either due to fracturing of the hinges along the axial-plane or indicates strain-slip in the same direction.

PLATE IV.1



Crenulation cleavage ( $S_2$ ) due to micro-folding (gneiss from Dyolidanda hill)

## Linear structures

### 1. Axes of minor folds

To this category belong (i) axes of small mesoscopic folds in quartzites (belonging to  $F_1$  and  $F_2$ ) and in schists (belonging to  $F_2$  and  $F_3$ ) and (ii) axes of microfolds, crinkles and puckers developed during the  $F_2$  and  $F_3$  folds.

### 2. Quartz rods and mullions

These are imperfectly preserved cores of folded quartz veins in micaceous rocks, and occur as distinct rods in mica-schists. Very often the intense folding of quartzite layers in schists have given rise to 'fold mullions'. This lineation mostly comprises that related to  $F_1$ . Occasional quartz-rods have developed during  $F_2$  also.

### 3. S-surface intersection

This lineation type belongs to two categories. One is that seen in flaggy quartzites, where the intersection of cleavage ( $S_1$ ) with bedding planes (S) has given rise to a fine striping or ribbons. Recrystallisation having partly obliterated this intersection, the lineation is seen as an ill-defined but conspicuous striation. This lineation is related to the  $F_1$  folding. The other category

comprises the intersection of the schistosity ( $S_1$ ) with the crenulation cleavage ( $S_2$ ). This  $S_1$ - $S_2$  intersection is rather sporadic.

### STRUCTURAL ELEMENTS RELATED TO VARIOUS EPISODES

#### Minor structures related to load

##### Planar structures:

- |                                   |   |     |
|-----------------------------------|---|-----|
| a) <u>Bedding and some relict</u> | } | (S) |
| <u>earliest schistosity</u>       |   |     |
| b) <u>Linear structures</u>       | - | Nil |

#### Minor structures related to the first folding

##### (Fold Episode - I)

##### a) Planar structures:

- |                                 |   |                   |
|---------------------------------|---|-------------------|
| i) Schistosity and gneissic     | } | (S <sub>1</sub> ) |
| foliation                       |   |                   |
| ii) Axial-planes of minor folds |   |                   |

##### b) Linear structures:

- |                                      |   |                   |
|--------------------------------------|---|-------------------|
| i) Axes of minor folds in quartzites | } | (L <sub>1</sub> ) |
| ii) Quartz rods and fold mullions    |   |                   |
| iii) Mineral orientation             |   |                   |
| iv) Striping, ribbons and striations |   |                   |
| v) S-surface intersection            |   |                   |

Minor structures related to the Second folding  
(Fold Episode - II)

a) Planar structures:

- |   |   |                   |
|---|---|-------------------|
| i) Axial-planes of the microfolds<br>and crenulations | ) | (S <sub>2</sub> ) |
| ii) Related strain-slip cleavage                      | ) |                   |

b) Linear structures:

- |  |   |                   |
|--|---|-------------------|
| i) Axes of the microfolds and<br>puckers                       | ) | (L <sub>2</sub> ) |
| ii) Axes of the folded quartz veins<br>and refolded quartzites | ) |                   |
| iii) Intersection of S <sub>1</sub> and S <sub>2</sub>         | ) |                   |

Minor structures related to the third folding  
(Fold Episode - III)

a) Planar structures:

- |  |   |                   |
|--|---|-------------------|
| i) Axial-planes of the minor folds<br>and faint crenulations | ) | (S <sub>3</sub> ) |
|--|---|-------------------|

b) Linear structures:

- |  |   |                   |
|--|---|-------------------|
| i) Axes of crenulations and<br>puckers in schists                | ) | (L <sub>3</sub> ) |
| ii) Axes of minor folds in quartzite<br>bands, rods and mullions | ) |                   |

### Minor structures related to the load

Bedding and bedding schistosity (S): Merh and Vashi (1965) and Vashi (1966) suggested that the main schistosity of the micaceous rocks of Almora Nappe was the earliest, and of axial-plane type, having originated by the metamorphism of the sediments during the isoclinal folding  $F_1$ . But observations of the author in Almora area, point to the existence of an earlier foliation, which got crenulated and tightly folded during the  $F_1$  folding giving rise to a new cleavage of axial-plane type. The author believes that perhaps this early foliation was a product of load, having developed prior to  $F_1$  folding. In their present state the rocks show only a sporadic preservation of this load schistosity (Plate IV.2). The behaviour of the earliest planar structure, is however ideally shown by the folded quartzite layers, whose bedding planes coincide with the load schistosity (S).

### Minor structures related to the $F_1$ folding

Planar structures: The present schistosity ( $S_1$ ) of the rocks, which comprises the main foliation is seen to be connected with the large scale reclined folding that synchronised with the main event of progressive regional metamorphism. The schistosity typically shows axial-plane



PLATE IV.2

Crinkling related to  $F_1$  in schists  
(Dyolidanda fold core)

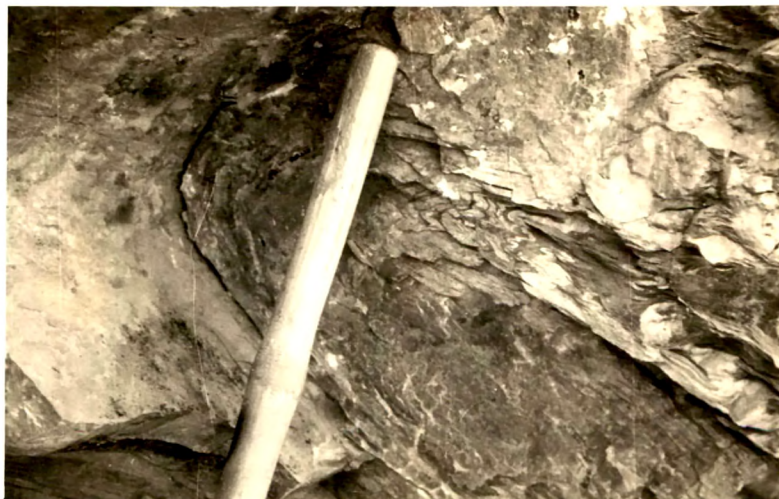
relation with the small quartzite folds (Plate IV.3).

At several places this axial-plane cleavage ( $S_1$ ) is seen to have developed by the tight microfolding of the early foliation (S). The apparent parallelism between the lithological banding and the schistosity ( $S_1$ ) is on account of the tight isoclinal nature of the  $F_1$  folding. Petrographic studies have also revealed that the schistosity is not a phenomenon of simple compression, but shearing stresses have also played a role in its development. Dominance of shearing stress is shown by snowball garnets in schists. Rolled garnets indicate differential slipping along the foliation during its crystallisation.

The gneissic foliation too has been included in this category, because it has been found that the gneisses are derived by the granitisation of mica-schists. Thus the foliation of gneisses is genetically the same as the schistosity.

Linear structures: They are mostly parallel to the fold axis, and comprise (1) axes of minor folds (2) S and  $S_1$  intersection and (3) mineral orientation. The different lineations described below show variable plunge in directions between NNW to NNE and SW.



PLATE IV.3

F<sub>1</sub> reclined fold in flaggy quartzite,  
micaceous layers showing axial-plane  
schistosity (Loc. south of Chaunsali)

(i) The most prominent and common linear structure, is the axes of minor folds of quartzites in schists. Folded quartz veins also form rods and mullions whose orientation coincides with the  $F_1$  fold axis.

(ii) Lineation  $L_1$  is also represented by a dimensional orientation of minerals. Streakiness on account of the orientation of elongated quartz grains, mica flakes and tourmaline needles (in gneisses) is included in this category. It appears that this lineation is due to the crystallisation of the above minerals along the fine cleavage - bedding intersections.

(iii) Ribbons, stripes and striations are common in the flaggy quartzites. The intersection of cleavage ( $S_1$ ) and bedding (S) has given rise to this lineation with the result that the quartzite surface (S) is marked by narrow flat stripes. Very often the recrystallisation has obscured the cleavage, and instead a prominent striping or striation has survived (Plate IV.4).

#### Minor structures related to the $F_2$ folding

Planar structures: These mainly consist of axial-planes of the microfolds and crenulations in schists, and this crinkling of  $S_1$  and development of microfolds on the



PLATE IV.4

L<sub>1</sub> lineation of striation type in flaggy  
quartzite (Loc. Khatari)

schistosity related to the  $F_2$  folding is observed throughout the area. At some places, the folding is so sharp that the hinges of the folds have broken, giving rise to a characteristic strain-slip cleavage along the axial-planes of the folds.

Linear structures: The fold axes of the microfolds and crenulations in schists characterise the lineation ( $L_2$ ), which at most places is recognised as a strong puckering of the schistosity surface. Axes of mesoscopic  $F_2$  folds in quartzites also indicate this lineation. Occasionally, this lineation ( $L_2$ ) is characterised by a streakiness due to the intersection of  $S_1$  and  $S_2$ . The  $L_2$  lineation plunges very gently in various directions between W,NW, ENE, E and ESE. Sometimes it is sub-horizontal.

Minor structures related to the  $F_3$  folding

Planar structures: This last folding episode has given rise to sporadic microfolds and puckers, whose axial planes characterise the planar structures  $S_3$ .

Linear structures: The axes of  $F_3$  microfolds and the faint puckers on schistosity ( $S_1$ ) showing northerly to north easterly plunge are recorded in the schists.

The axes of a few conspicuous minor folds of  $F_3$  generation in quartzites, also characterise the lineation  $L_3$ .

### STRUCTURAL ANALYSIS

The area having undergone several fold episodes, in its most parts, structures of more than one generation occur together. Minor structures belonging to various fold episodes have generally different characteristic styles as shown by minor folds and lineation types. They were carefully identified and sorted out. At many places, the rocks show fold interference patterns due to superimposition of late structures over earlier ones. These interference patterns mostly comprise refolded folds and folded lineations (Plate IV.5) and cleavages.

The whole area was subdivided into 18 sub-areas (Fig.IV.2) and the foliation planes and linear structures from each unit in turn, were plotted on and analysed with the help of schmidt equal area net. For the purpose of relating linear structures to major folds, a number of  $\pi$ - diagrams were prepared. The usefulness and importance of these stereograms will be evident from the sub-area wise description of the structural characters.



PLATE IV.5

$L_1$  ribbons folded by a small  $F_2$  fold  
in quartzite (Loc. Phalsimi)

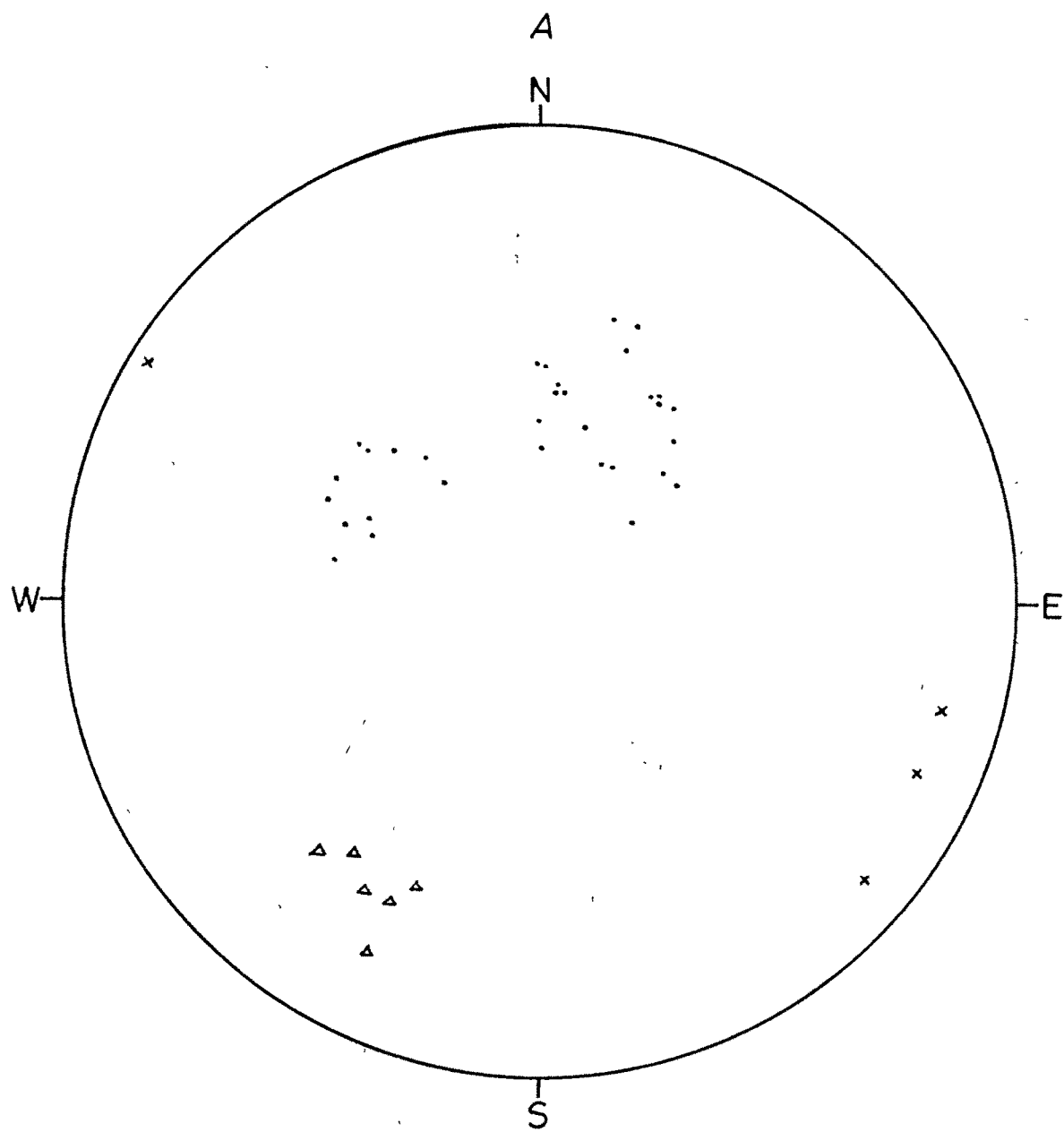
### Sub-area (1)

Lying in the north-eastern corner of the amp, this sub-area includes the rocks on the western half of the south dipping limb of Dinapani-Kaparkhan synform. The rock types are mica-schists with layers of quartzites. The schistosity and the quartzite bedding, which are more or less parallel to each other, dip due S, their strikes fluctuate between NW-SE to E-W. This sub-area shows the effect of  $F_3$ , and in the contoured  $\pi$  - diagram a fragmentary girdle indicates this folding, the pole of the girdle being the  $F_3$  fold axis.  $L_3$  lineations related to  $F_3$  are not recorded. Lineations  $L_1$  and  $L_2$  related to  $F_1$  and  $F_2$  respectively, are occasionally encountered.  $L_1$  lineations show moderate plunge between  $S20^\circ W$  to  $S45^\circ W$ . Stray  $L_2$  lineations show very gentle plunge between  $S52^\circ E$  to  $S75^\circ E$  and  $N60^\circ W$ , or is almost sub-horizontal (Fig.IV.4A-B).

### Sub-area (2)

This sub-area forms the north-western corner, lying to the east of sub-area (1). The rock types are as usual garnet mica-schists and quartzites. This also forms a portion of the south dipping limb of the Dinapani-Kaparkhan synform. The foliation trend shows

# *Stereograms showing the stru*



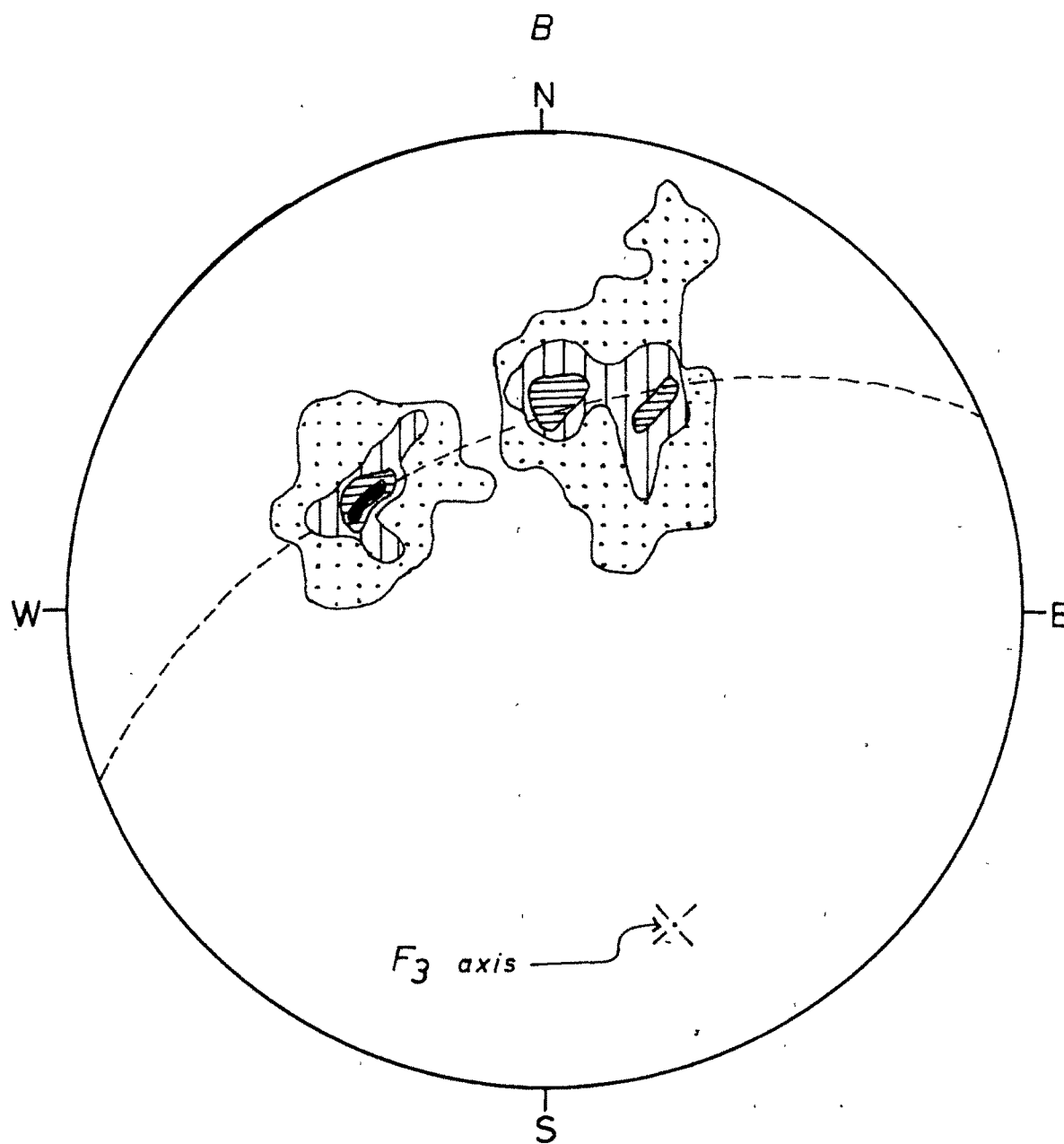
• Poles of foliation (36)

△  $L_1$  Lineations (6)


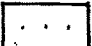

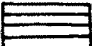

×  $L_2$  Lineations (4)



ctural elements of the sub-area 1.



Contour intervals :-

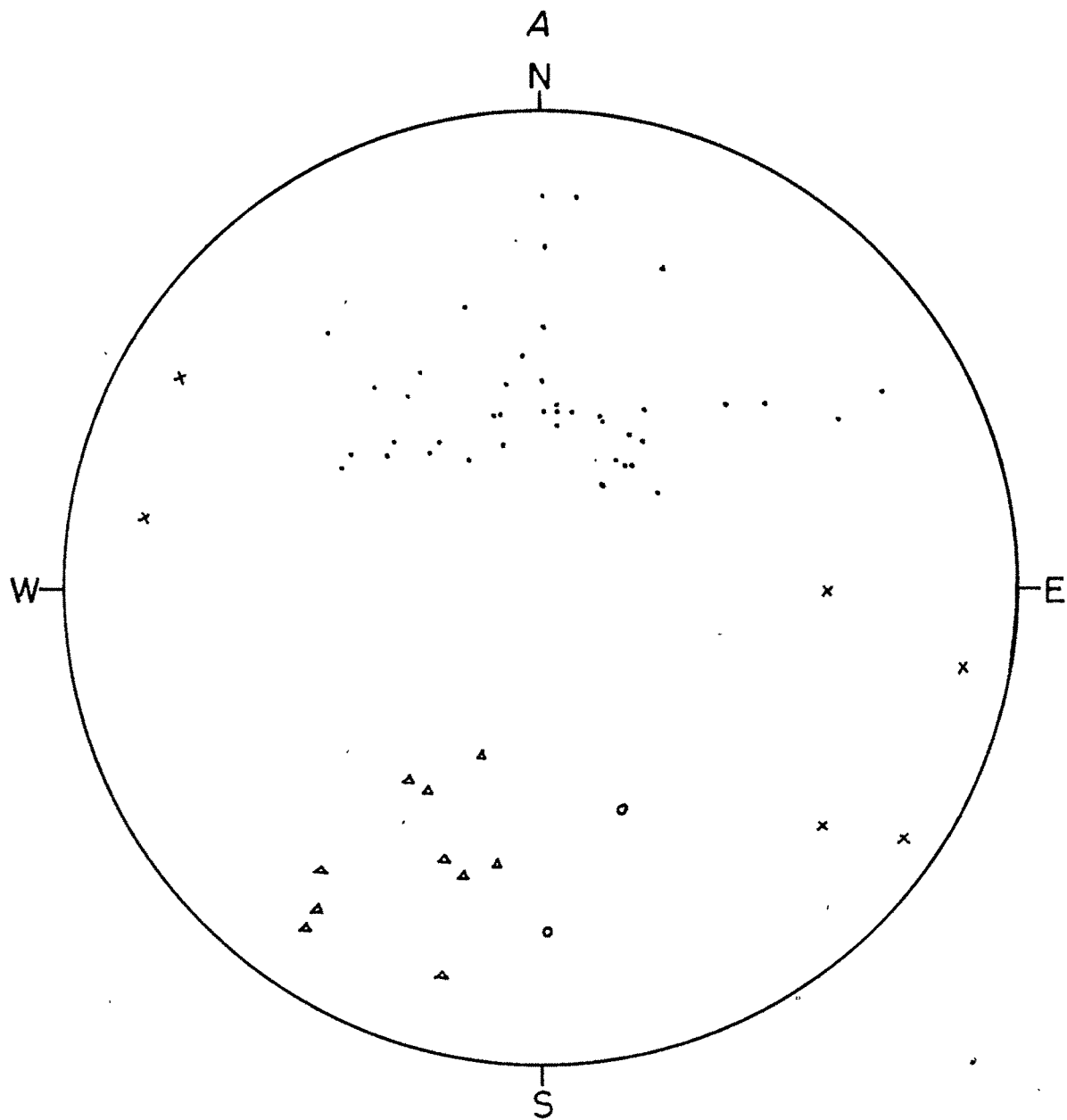
	0 - 1 %
	1 - 3 %
	3 - 5 %
	5 - 7 %
	> 7 %

$F_3$  flexures and this fact comes out quite clearly on the contoured  $\pi$  - diagram. The stereogram shows a tendency to form two fragmentary girdles, each representing two orientations of the schistosity (due to  $F_2$ ) having been folded on  $F_3$ . Only two  $L_3$  lineations related to  $F_3$  are recorded.  $L_1$  lineation shows moderate plunge between  $S15^\circ W$  to  $S45^\circ W$ . The  $L_2$  lineation shows gentle plunge in both NW and SE quadrants (Fig.IV.5A-B).

### Sub-area (3)

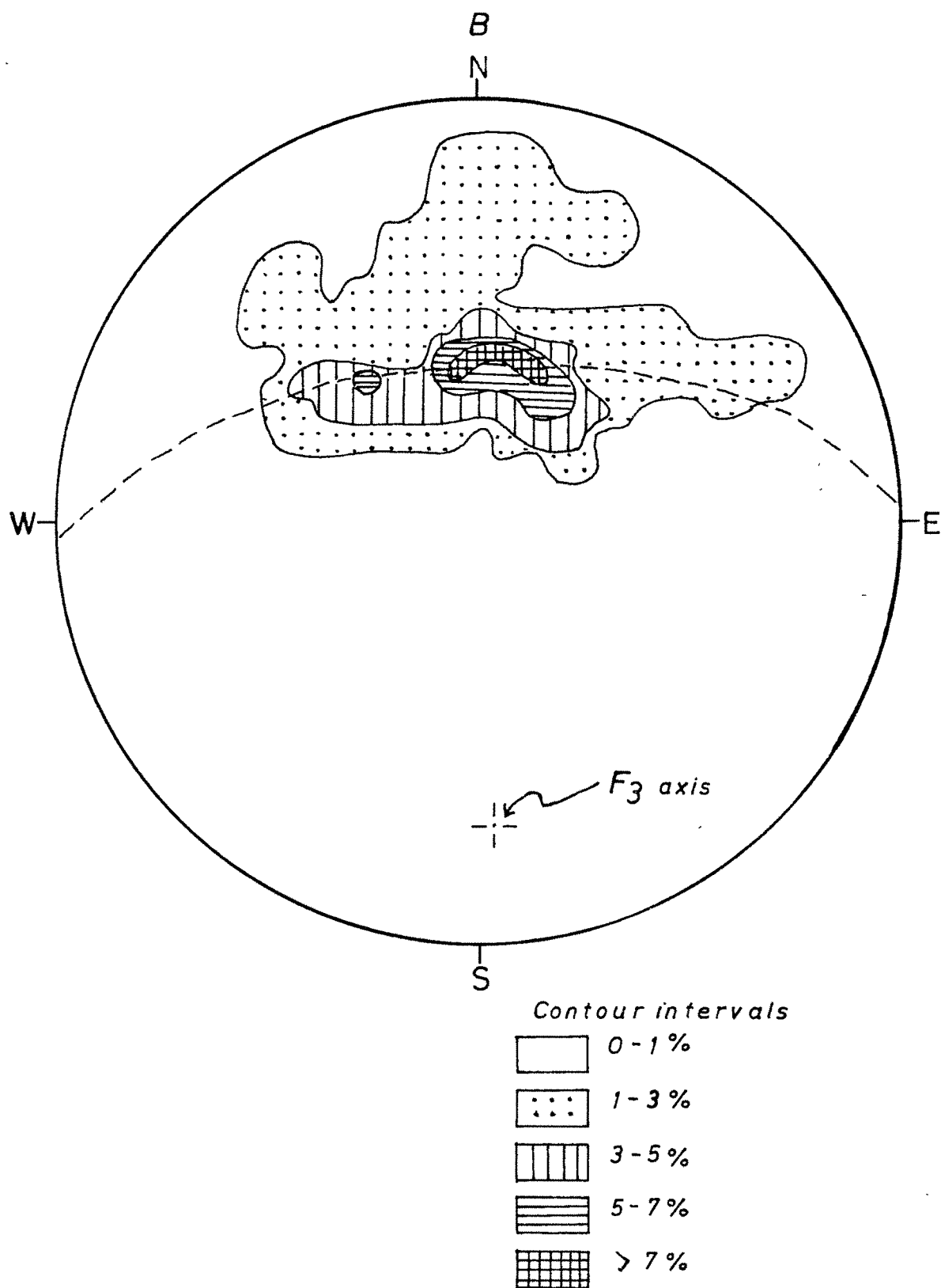
In the north-eastern corner of the map, this sub-area, lies to the south of the sub-area (2) across the synformal axis, and contains rocks of the southern limb, mainly garnet mica-schists and quartzites. This sub-area shows very pronounced effect of  $F_3$  folding, which has an almost NE-SW axial trend. The entire sub-area comprises a number of mesoscopic  $F_3$  folds. The  $\pi$  -diagram shows a distinct *girdle* due to  $F_3$ , whose pole characterises the  $F_3$  axis. Related  $L_3$  lineations show moderate plunge due NE.  $L_1$  and  $L_2$  are sporadically present.  $L_1$  plunges due  $N12^\circ W$  to  $N30^\circ W$ , while the  $L_2$  shows a gentle to moderate plunge towards  $N80^\circ E$  to  $S80^\circ E$  and towards W (Fig.IV.6A-B).

## *Stereograms showing the str*

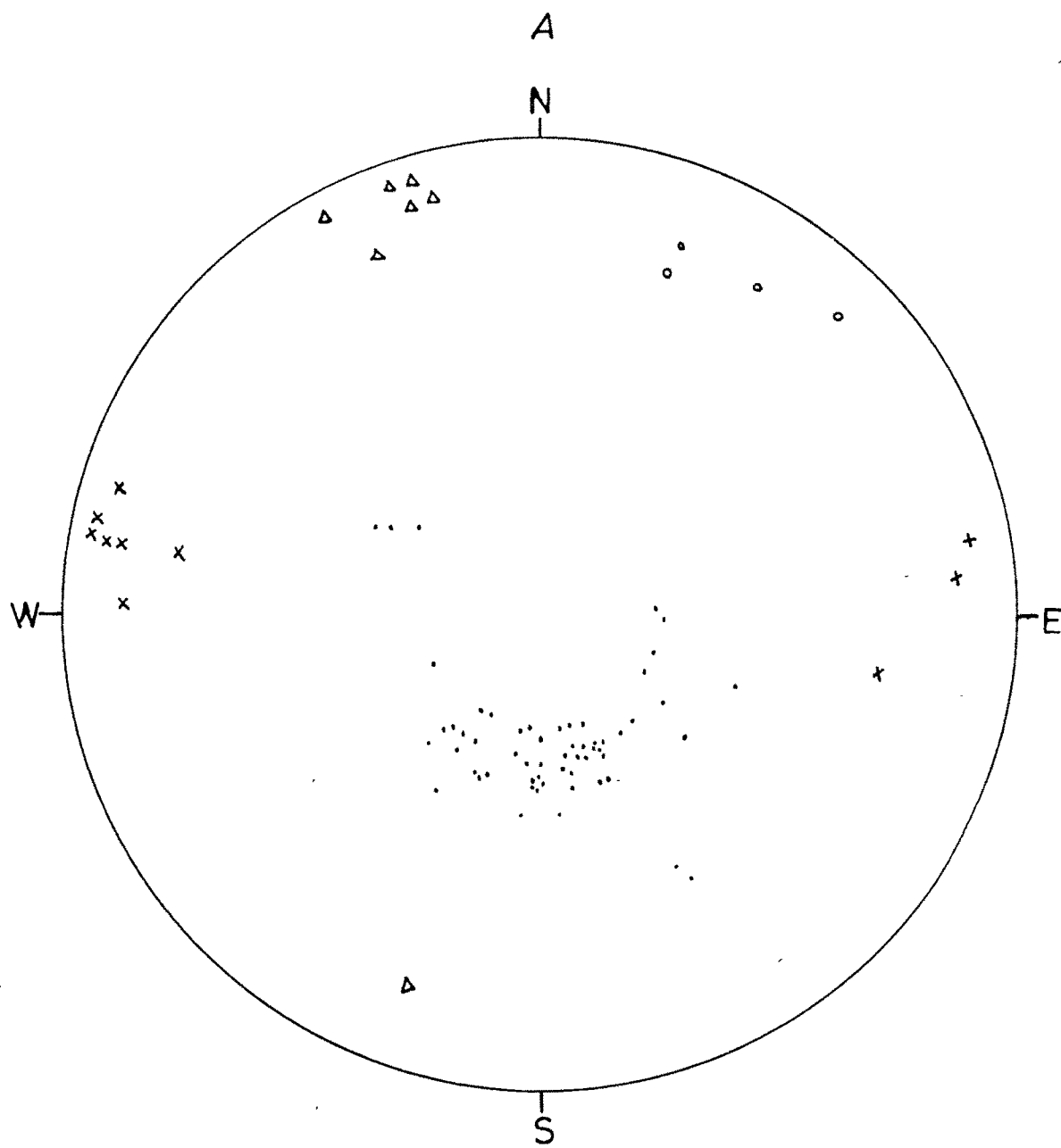


- Poles of foliation (42)
- Δ *L*<sub>1</sub> Lineations (10)
- x *L*<sub>2</sub> Lineations (6)
- *L*<sub>3</sub> Lineations (2)

Structural elements of the sub-area 2.



# *Stereograms showing the str*

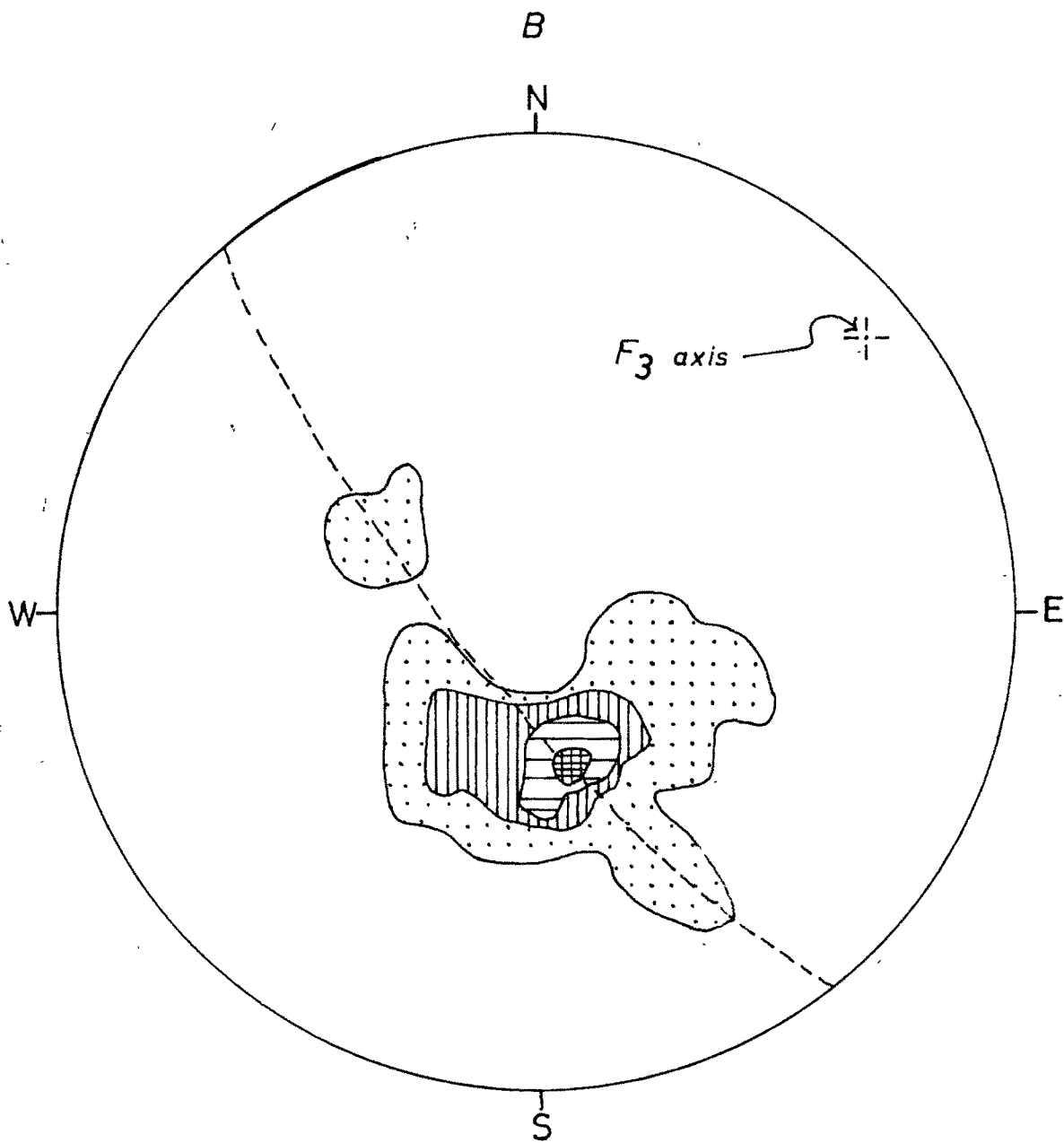


- Poles of foliation (58)
- Δ  $L_1$  Lineations (7)
- x  $L_2$  Lineations (10)
- $L_3$  Lineations (4)

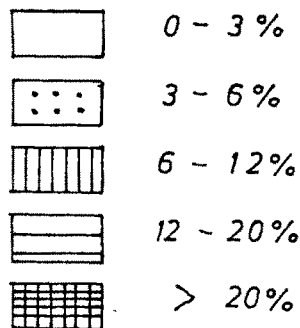
Fig. IV. 6.

83

Structural elements of the sub area 3.



Contour intervals



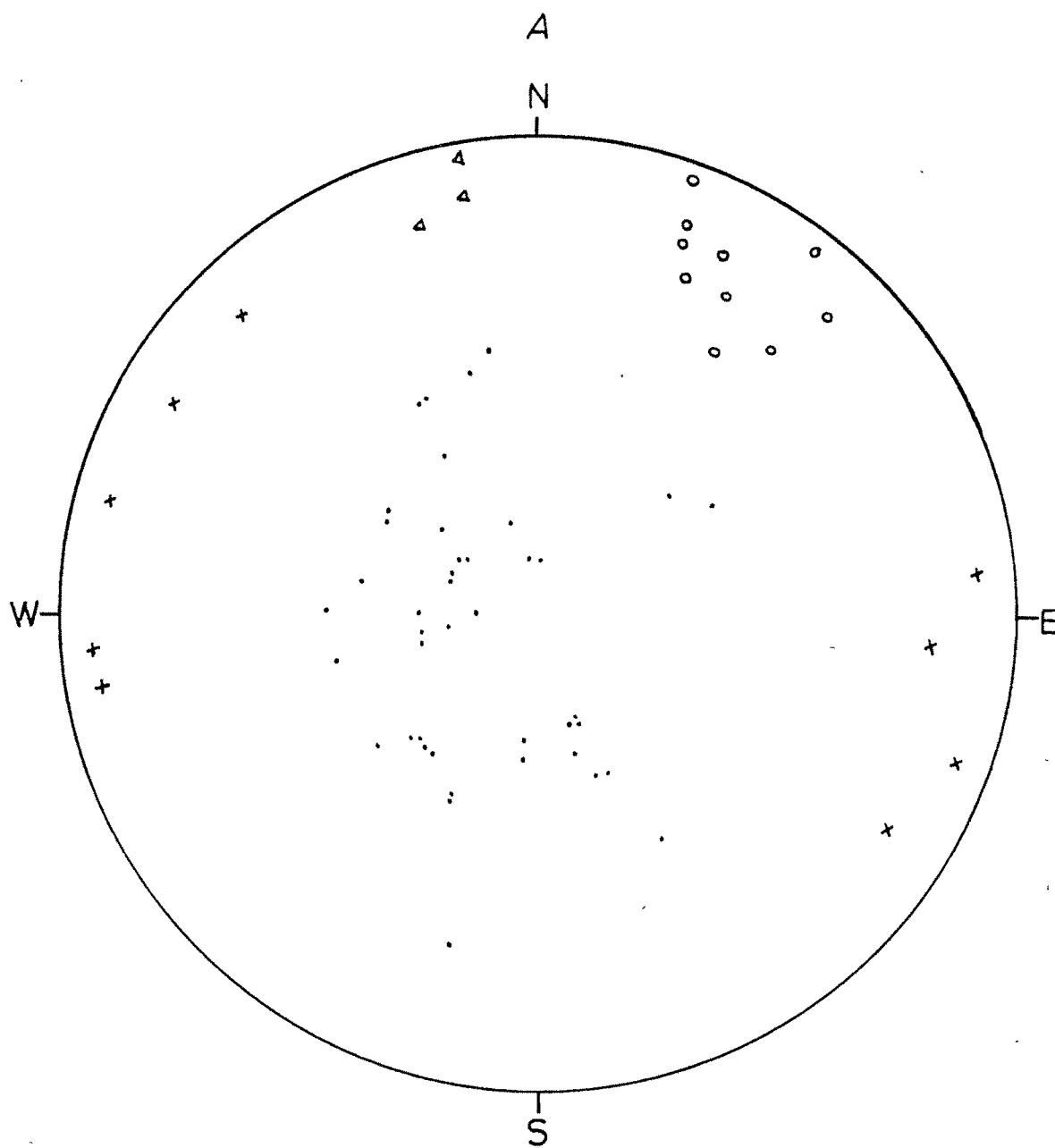
#### Sub-area (4)

In the north-eastern corner, the sub-area (4) includes a portion of actual hinge area of the Dinapani-Kaparkhan synform. The rocks, generally garnet mica-schists with quartzite layers, show very conspicuous effects of the superimposition of  $F_3$  on  $F_2$ , on a macroscopic scale. The northern limb is less affected by  $F_3$  but the southern limb is considerably distorted, forming an arch-shaped antiform, plunging north-eastward. The stereogram of the foliation typically shows a pattern that can be resolved into 2 well formed girdles I and II and one fragmentary girdle III. The girdle I is due to  $F_2$ , while the II and III are due to  $F_3$  - the former comprises the antiformal flexure on the southern limb, while the latter indicate a less evident  $F_3$  flexure on the northern limb of the synform.  $L_3$  lineations related to the girdle II show north-easterly plunge.  $L_1$  plunges due  $N15^\circ W$  or  $S10^\circ W$ , while  $L_2$  has the usual gentle plunge ranging between  $N85^\circ E$  to  $S60^\circ E$  or  $N35^\circ W$  to  $S80^\circ W$  (Fig. IV.7A-B).

#### Sub area (5)





This sub-area lies to the SW of sub-area (4) and its rocks, the usual garnet mica-schists, quartzites and graphitic schists show very distinct impress of  $F_1$  and  $F_3$ .

# *Stereograms showing the*



- Poles of foliation (42)
- Δ  $L_1$  Lineations (3)
- x  $L_2$  Lineations (9)
- $L_3$  Lineations (10)



	0 - 1%
	1 - 3%
	3 - 5%
	> 5%

On the stereogram, only the effect of  $F_3$  flexuring comes out, being indicated by a fairly well defined girdle.  $L_1$  lineation shows a gentle plunge between  $N5^\circ W$  to  $N30^\circ W$ .  $L_2$  plunges gently both ways - between  $N70^\circ E$  to  $N80^\circ E$  and  $S70^\circ W$  to  $N70^\circ W$ . In this sub-area,  $L_3$  lineations is very distinct and shows a gentle plunge between  $N15^\circ E$  to  $N35^\circ E$  (Fig.IV.8A-B).

#### Sub-area (6)

This sub-area contains the rocks around the village Chitai, south of sub-area (3) and (5). Its rocks are mainly garnet mica-schists, quartzites and graphitic schists. The foliation trend shows much fluctuation due to  $F_3$  flexures though in all cases dipping northward. The quartzite outcrop ideally shows a macroscopic  $F_1$  fold closing to the NW. The northeastern limb of this  $F_1$  fold is folded into an  $F_3$  antiform (~~Plate IV.7~~). All the lineations  $L_1$ ,  $L_2$  and  $L_3$  are present. The  $L_1$  lineations show gentle plunge in directions varying between N and  $N15^\circ W$ . The  $L_2$  lineation shows the usual very gentle plunge, both due E and W. The east plunging lineation shows variation in its direction from  $N80^\circ E$  to  $S80^\circ E$ . The  $L_3$  lineation plunges moderately between  $N18^\circ E$  to  $N40^\circ E$ . The westerly plunging lineation shows variation in its direction from  $N85^\circ W$  to W. The  $\pi$ -diagram shows a faint girdle, the

## Stereograms showing the str

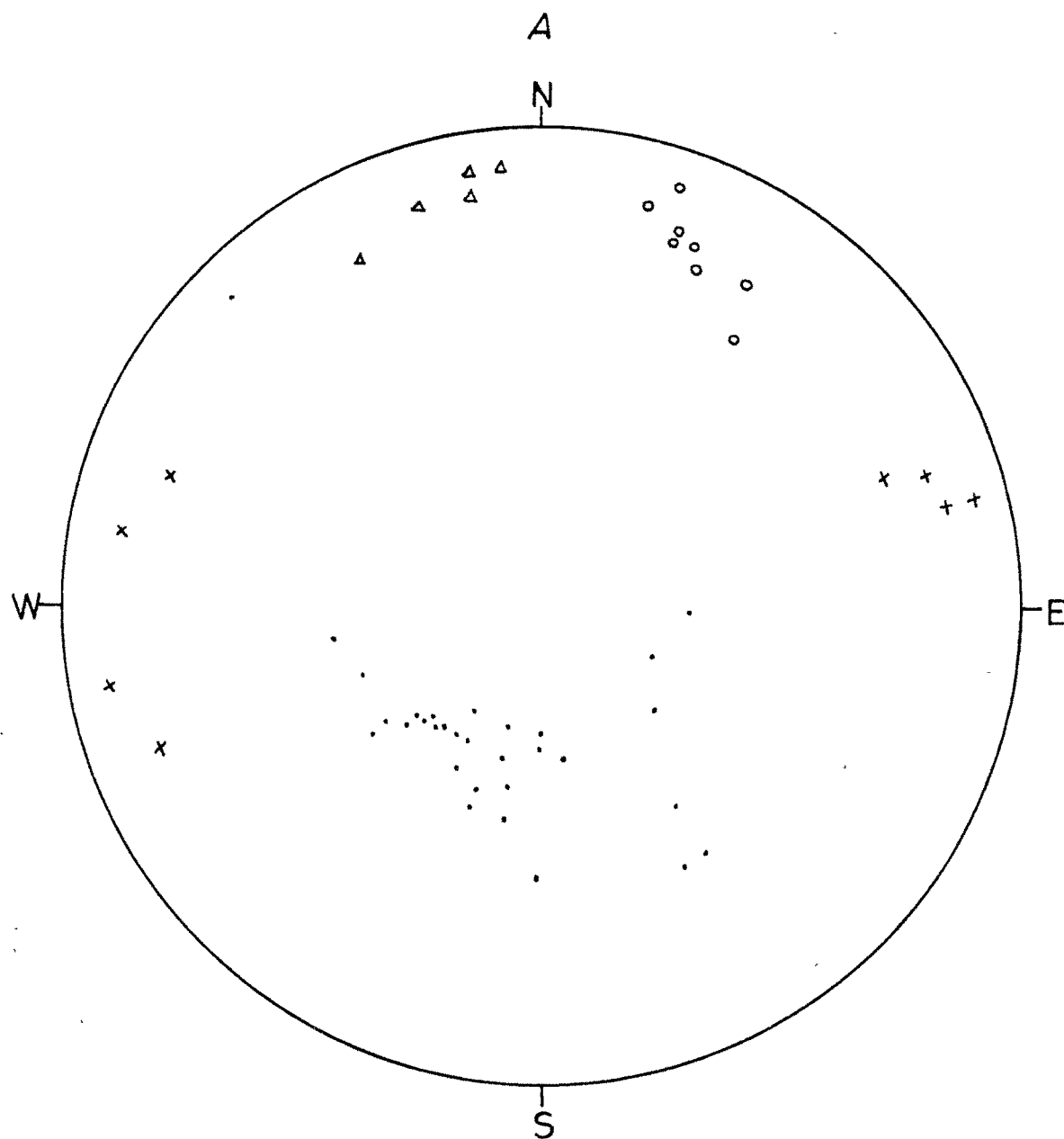
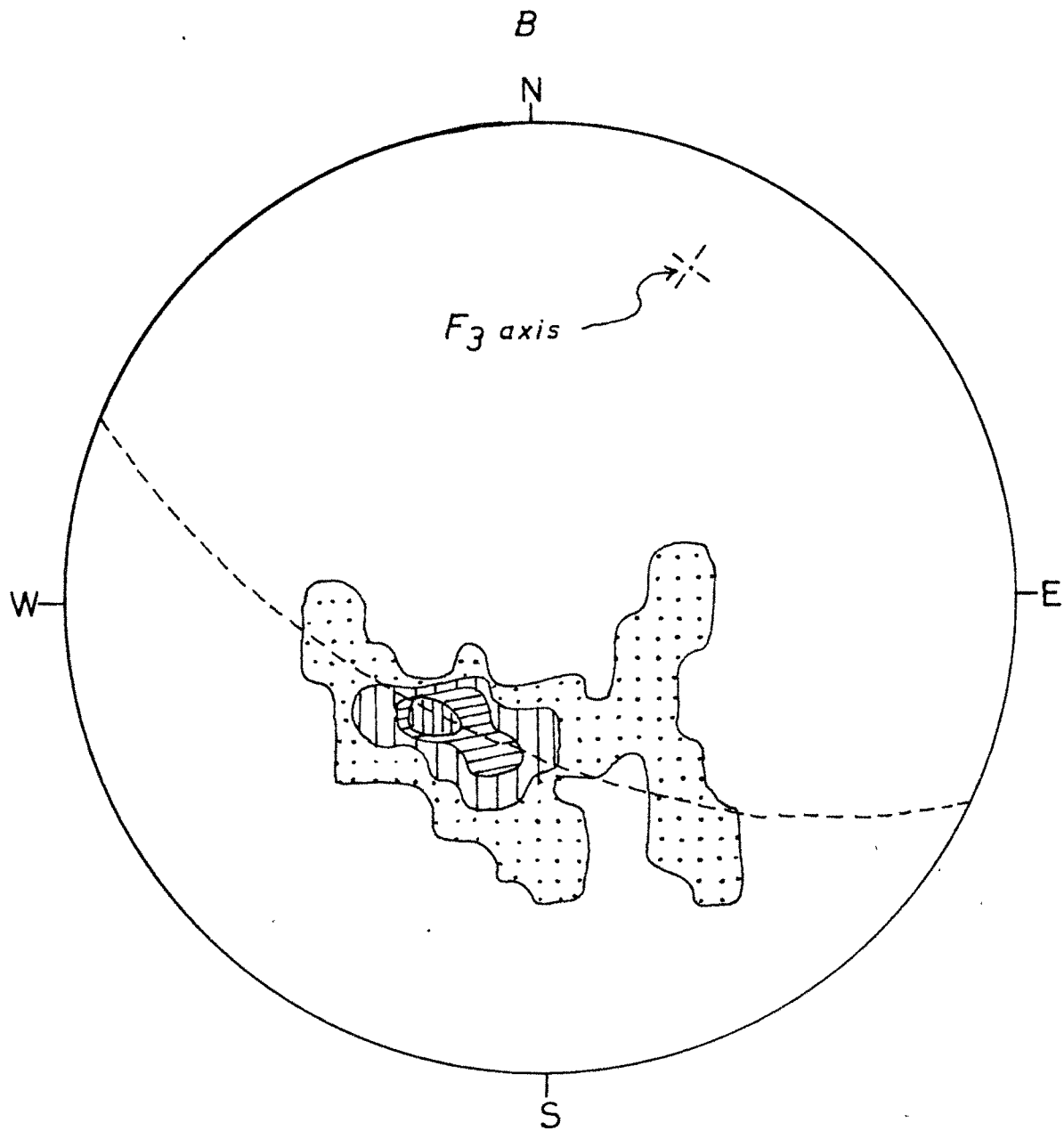



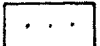

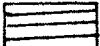

Fig. IV.8.

Structural elements of the sub-area 5.

87



Contour intervals :-

	0 - 1 %
	1 - 3 %
	3 - 5 %
	5 - 7 %
	> 7 %

pole of which coincides with the  $F_3$  axis, and it is obvious that the fluctuation in the strike directions is on account of  $F_3$  (Fig.IV.9A-B).

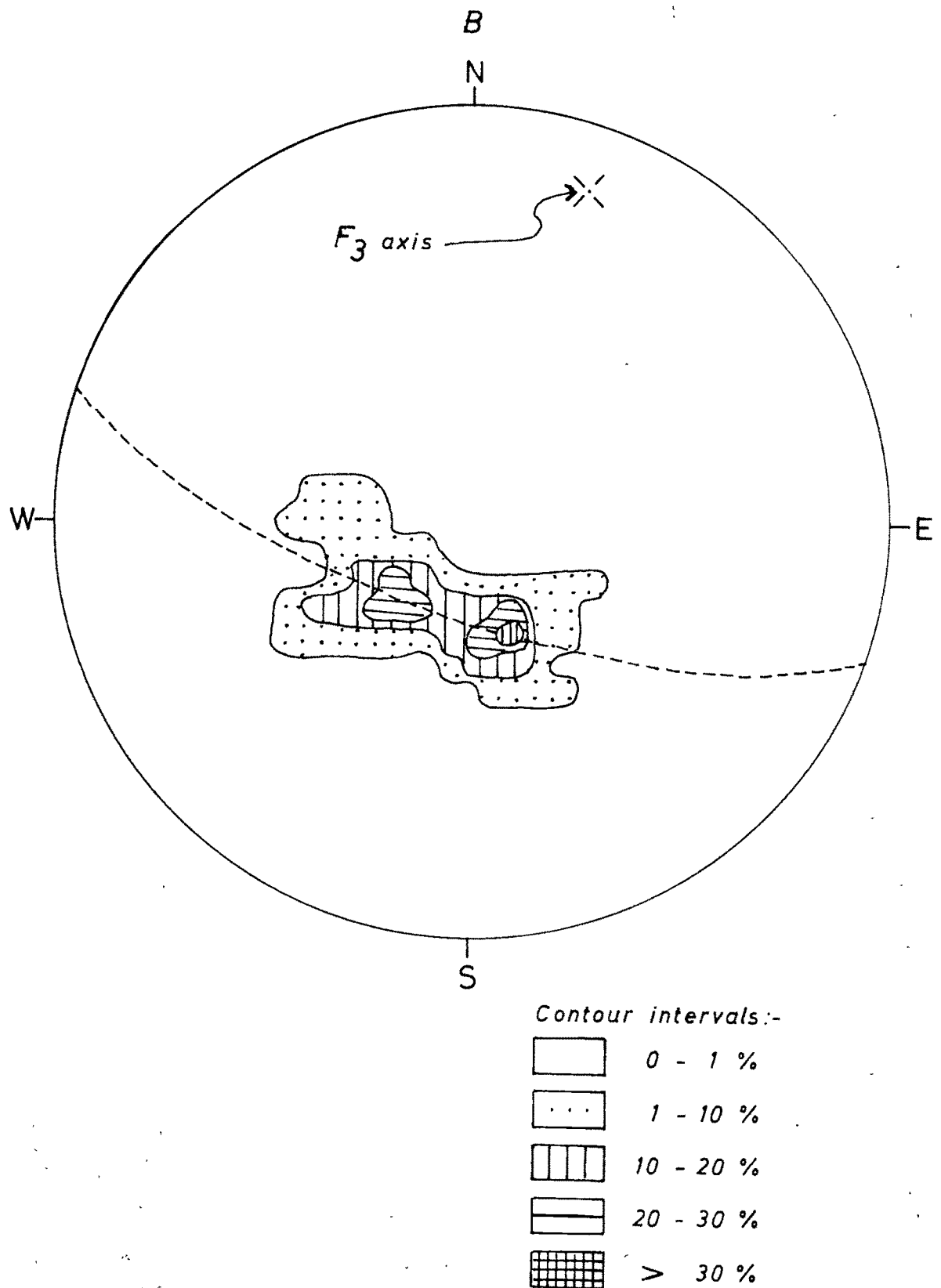
#### Sub-area (7)

This sub-area includes the ground to the south of sub-area (6). It contains several bands of quartzites in garnet mica-schists. The repetition of quartzites is obviously due to  $F_1$  folding. This sub-area exhibits superimposition of  $F_2$  on  $F_1$ . Large sized  $F_1$  folds have been refolded on  $F_2$  to give an antiform (Sual antiform) in this part of the study area, and this sub-area forms the northern limb of the antiform. Superimposition of  $F_3$  flexures has caused fluctuation in the strike of the NE dipping foliations. The contoured  $\pi$ -diagram shows a tendency for a girdle to mark the  $F_3$  flexures. Lineations of all the three generations are recorded.  $L_1$  shows a northerly plunge between  $N8^\circ W$  and  $N20^\circ E$ . The  $L_2$  lineation which is quite numerous, plunges with rather small angles towards  $N60^\circ E$ ,  $SSO^\circ E$  and  $W$ . The  $L_3$  lineation which has almost an identical orientation as  $L_1$ , is identified on the basis of its nature, and a slight difference in the direction of plunge between  $N18^\circ E$  to  $N42^\circ E$  (Fig.IV.10A-B).

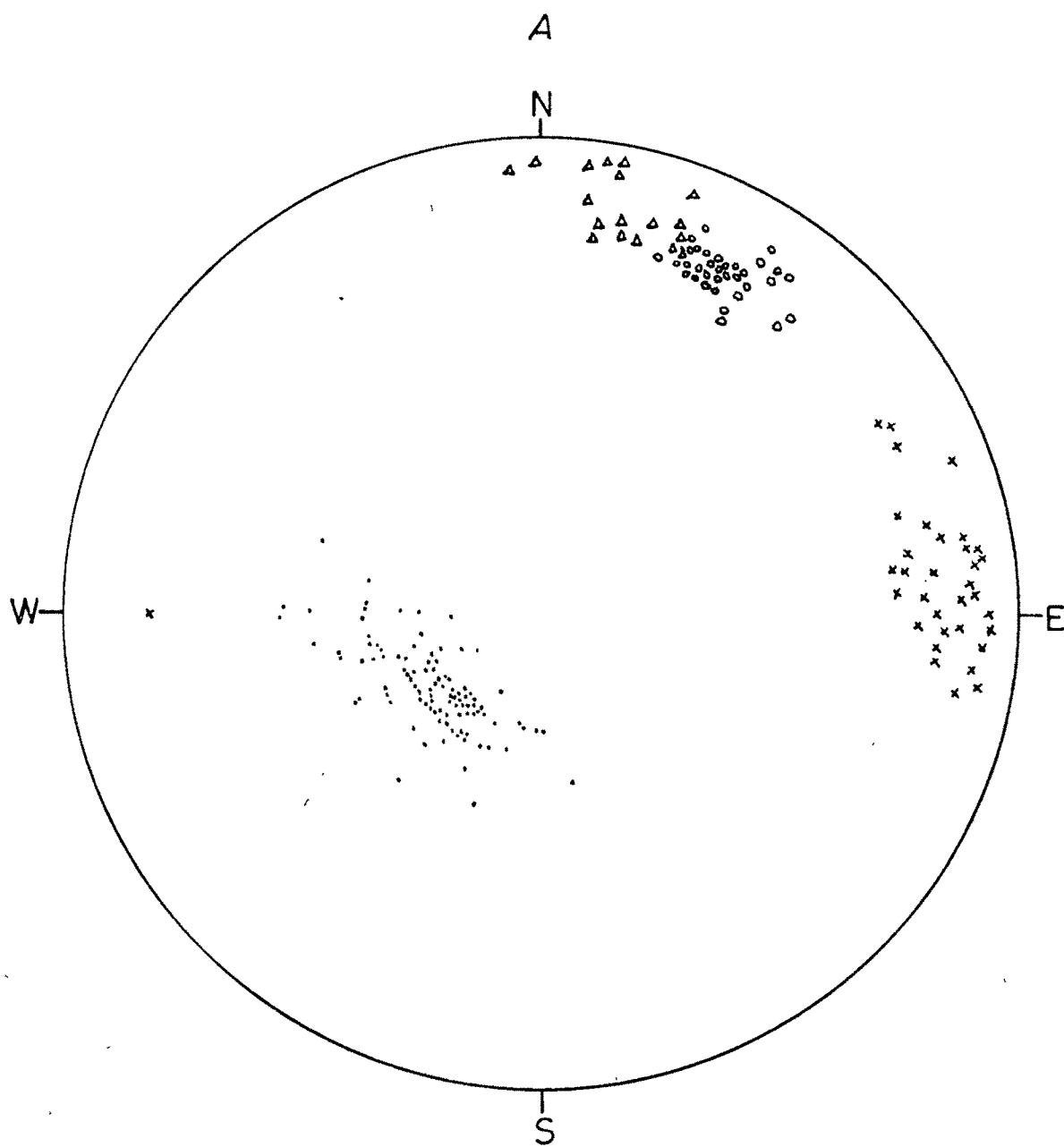
Fig. IV.9

structural elements of the sub area 6.

89

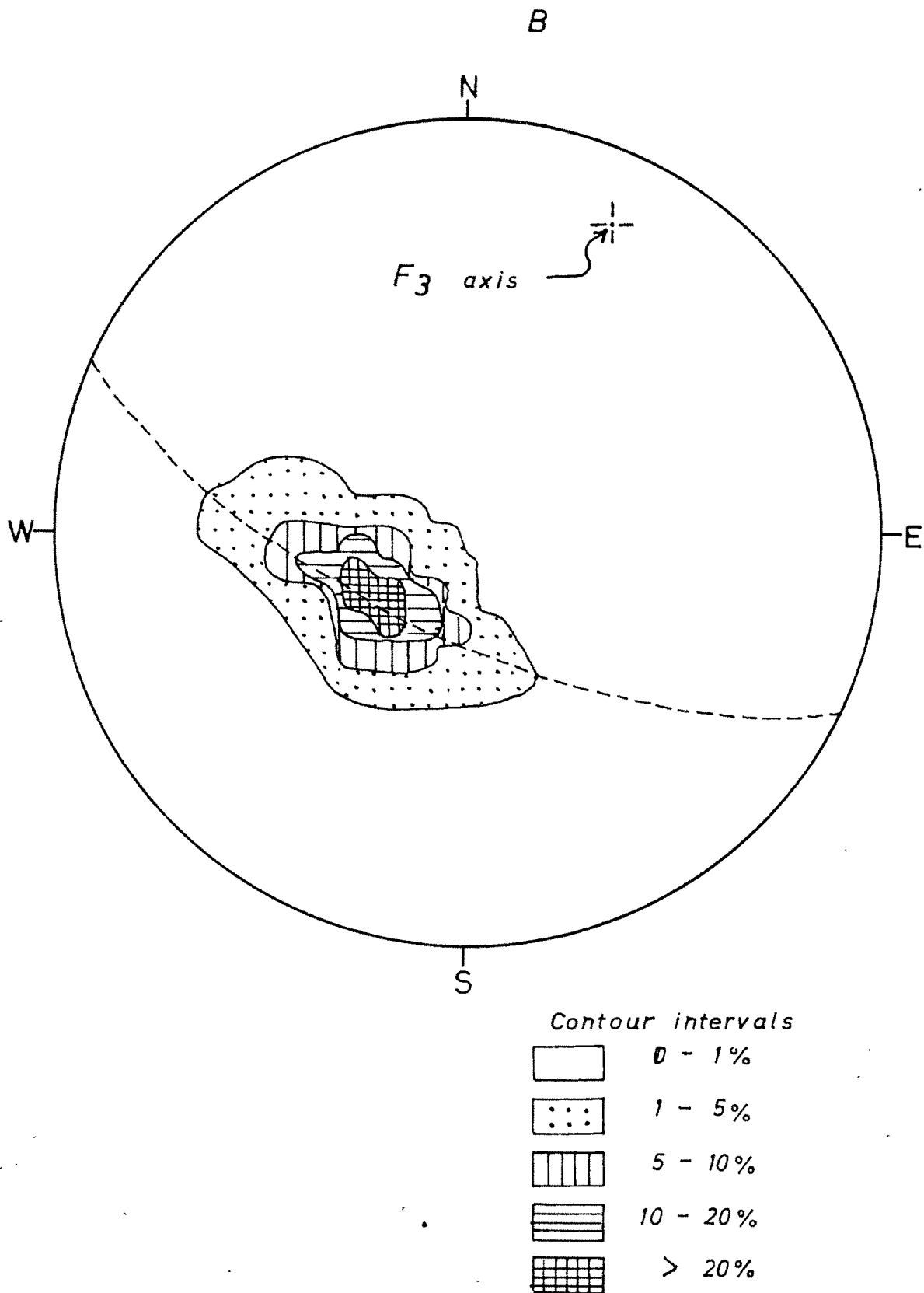


## *Stereograms showing the stru*



- Poles of foliation (150)
- Δ  $L_1$  Lineations (18)
- ×  $L_2$  Lineations (34)
- $L_3$  Lineations (33)

ctural elements of the sub-area 7.





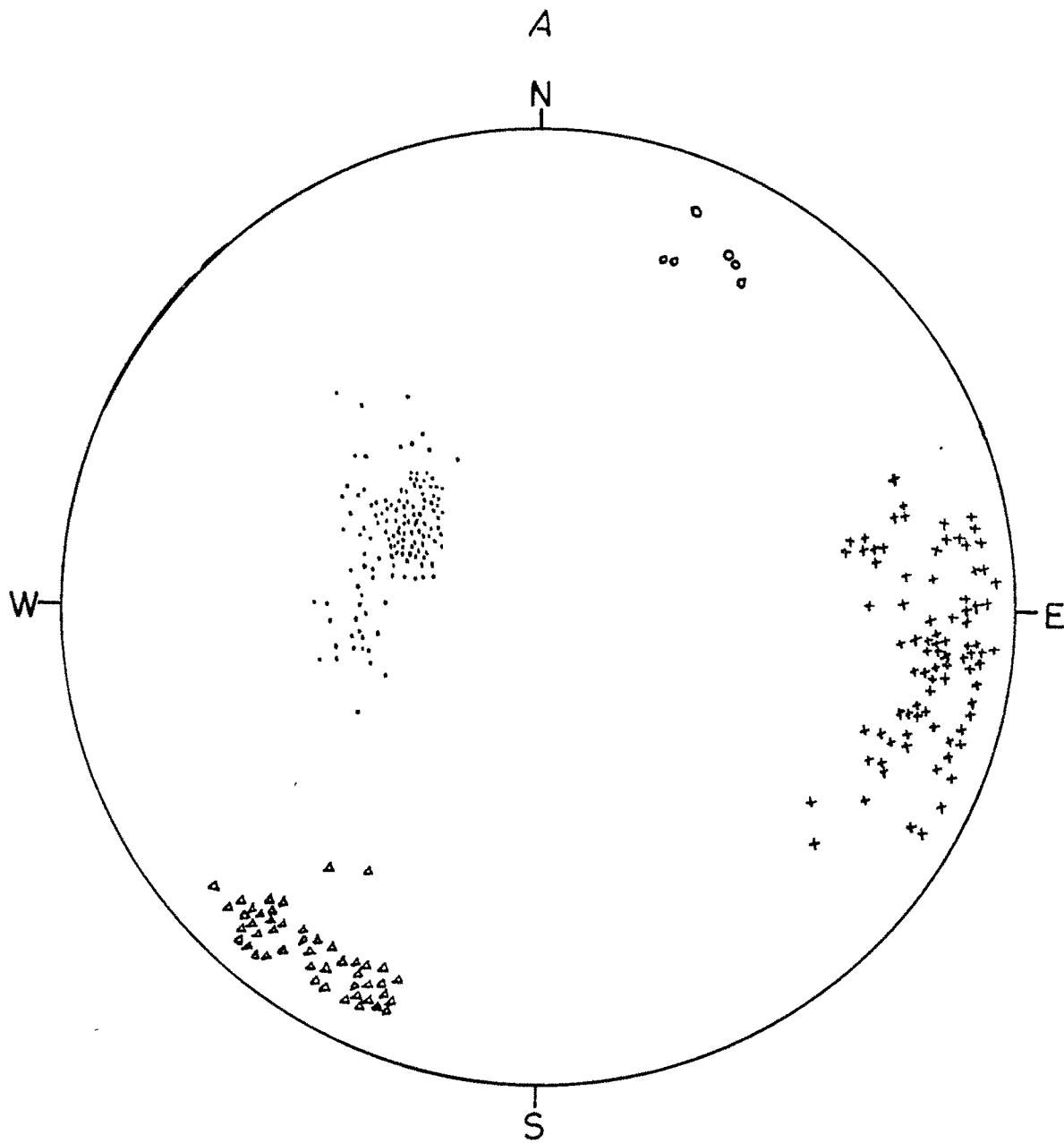
Sub-area (8)

Lying to the south of sub-area (7), it contains the ESE dipping southern limb of the Sual antiform. The rocks are mostly garnet mica-schists and graphitic schists, with a band of quartzite folded on  $F_1$  in the NE corner.  $L_1$  lineation is showing a plunge due  $S20^\circ W$  and  $S50^\circ W$ . This variation in the plunge direction is due to the effect of  $F_2$  fold.  $L_2$  lineations plunge gently, show variation in direction between  $N70^\circ E$  and  $S55^\circ E$ . The  $\mathcal{T}$ -diagram reveals a tendency of folding on  $F_2$ , the pole of the fragmentary girdle in a general way coinciding with  $L_2$  plots.  $L_3$  lineation is rather sporadic, and wherever noted, it has a plunge which varies between  $N20^\circ E$  and  $N30^\circ E$  (Fig.IV.11A-B).

Sub-area (9)

Further south of sub-area (8) the foliation swings to almost NW-SE and thus forms a complementary synform on  $F_2$  (Guna synform). The rocks are only garnet mica-schists and graphitic schists. This sub-area contains the southern limb of the synform. The dips are generally due NE. The  $\mathcal{T}$ -diagram does not reveal anything, except the dip and strike of the foliation.  $L_1$  lineations are not recorded, but the  $L_2$  and  $L_3$  lineations are abundant and show the usual orientation, plunging due  $N76^\circ E$  to  $S72^\circ E$  and  $N12^\circ E$  to  $N45^\circ E$  respectively (Fig.IV.12A-B).

# *Stereograms showing the struct*

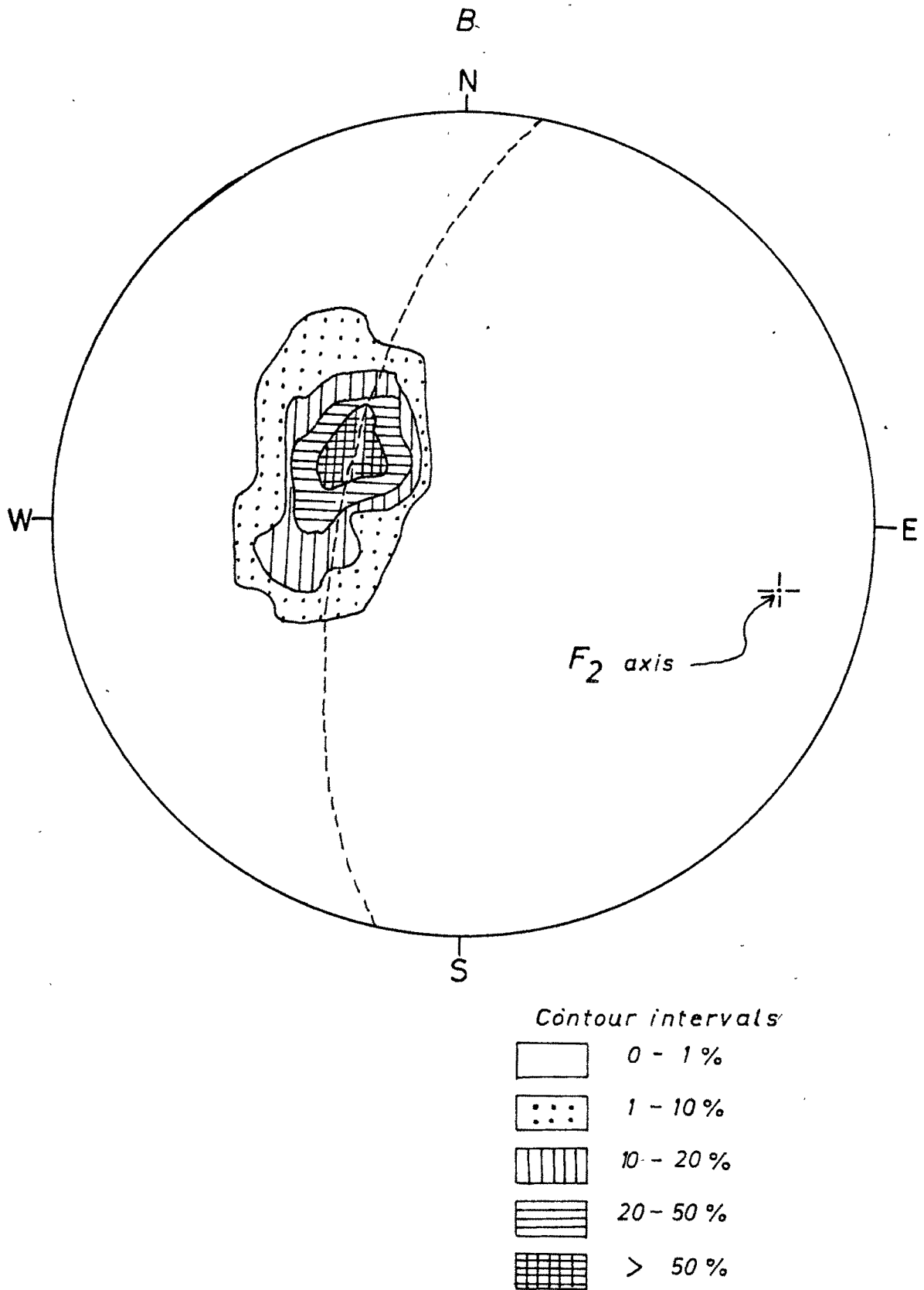


- *Poles of foliation (105)*
- Δ *L<sub>1</sub> Lineations (48)*
- × *L<sub>2</sub> Lineations (90)*
- *L<sub>3</sub> Lineations (6)*

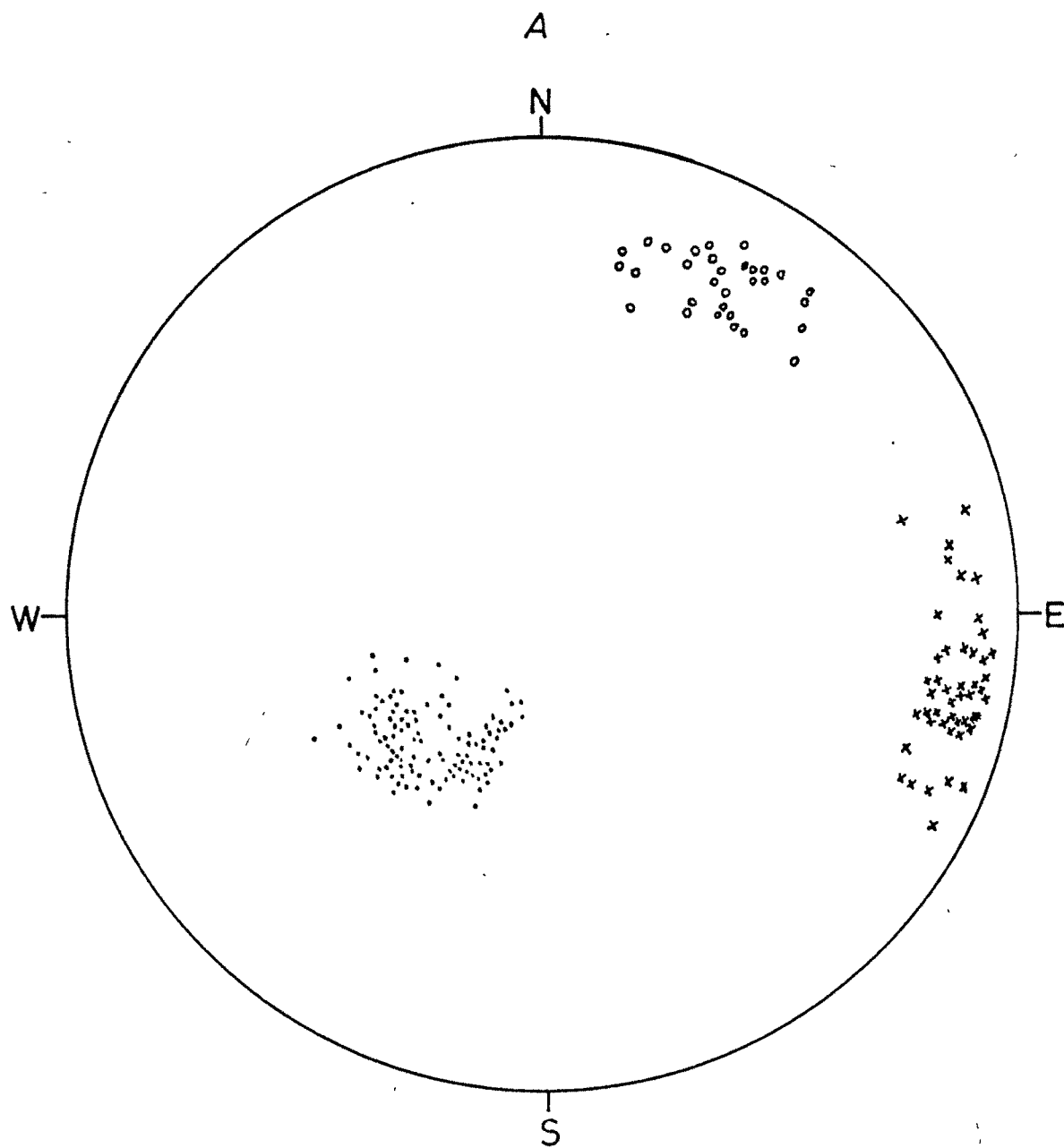
Fig. IV.11.

ural elements of the sub area 8.

92

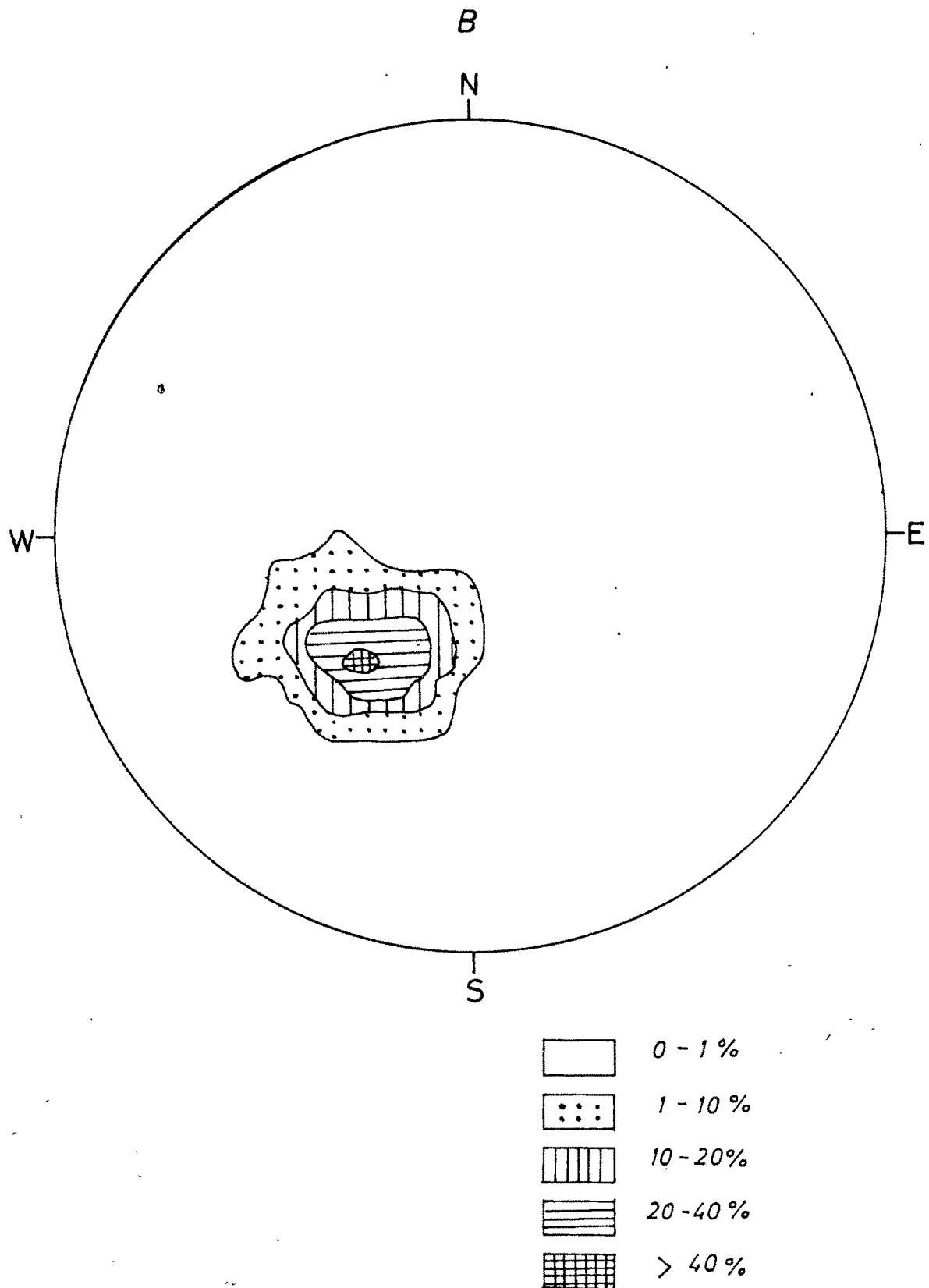


# *Stereograms showing the*



- Poles of foliation (105)
- x  $L_2$  Lineation (46)
- o  $L_3$  Lineation (31)

*structural elements of the sub area 9.*



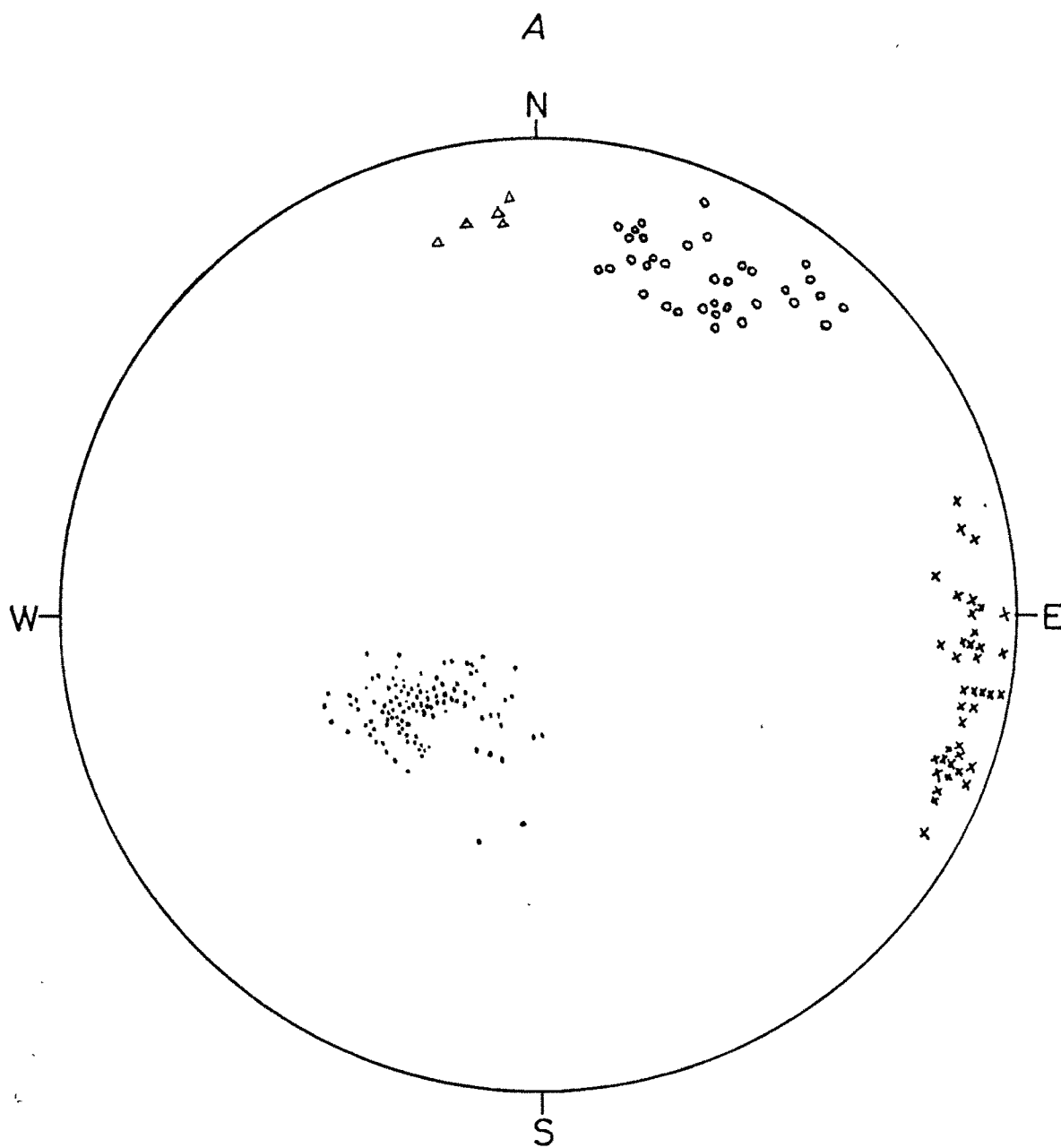
Sub-area (10)

This sub-area, to the west of sub-area (9), has structural characters ~~to~~ identical to those of the latter. The rocks are dominantly garnet mica-schists with a few subordinate quartzite bands. A part of the area is occupied by the gneisses in the NW. The foliation trends NW-SE and dips due NE. Its  $\mathcal{W}$ -diagram shows a point maxima, with no girdle. A few  $L_1$  lineations are recorded which plunge almost N to  $N15^\circ W$  at gentle angles.  $L_2$  lineations are quite numerous and show a scattering of plunge direction from  $N75^\circ E$  to  $S70^\circ E$ .  $L_3$  lineations are also abundantly recorded and it shows gentle to moderate plunge north eastward between  $N12^\circ E$  to  $N46^\circ E$  (Fig.IV.13A-B).

Sub-area (11)

The rocks of sub-area (11) lie to the north of sub-area (10) and consist of garnet mica-schists and quartzites. The foliation almost uniformly strikes NW-SE and dips at moderate angles to the NE. The outcrop pattern reveals existence of a couple of quartzite bands folded on  $F_1$  and the related  $L_1$  lineations vary in directions from  $N12^\circ E$  to  $N25^\circ E$ . Effect of  $F_2$  folding is not seen in the foliation trend, and only the lineations  $L_2$  are prominently developed which are seen showing an

# *Stereograms showing the st*



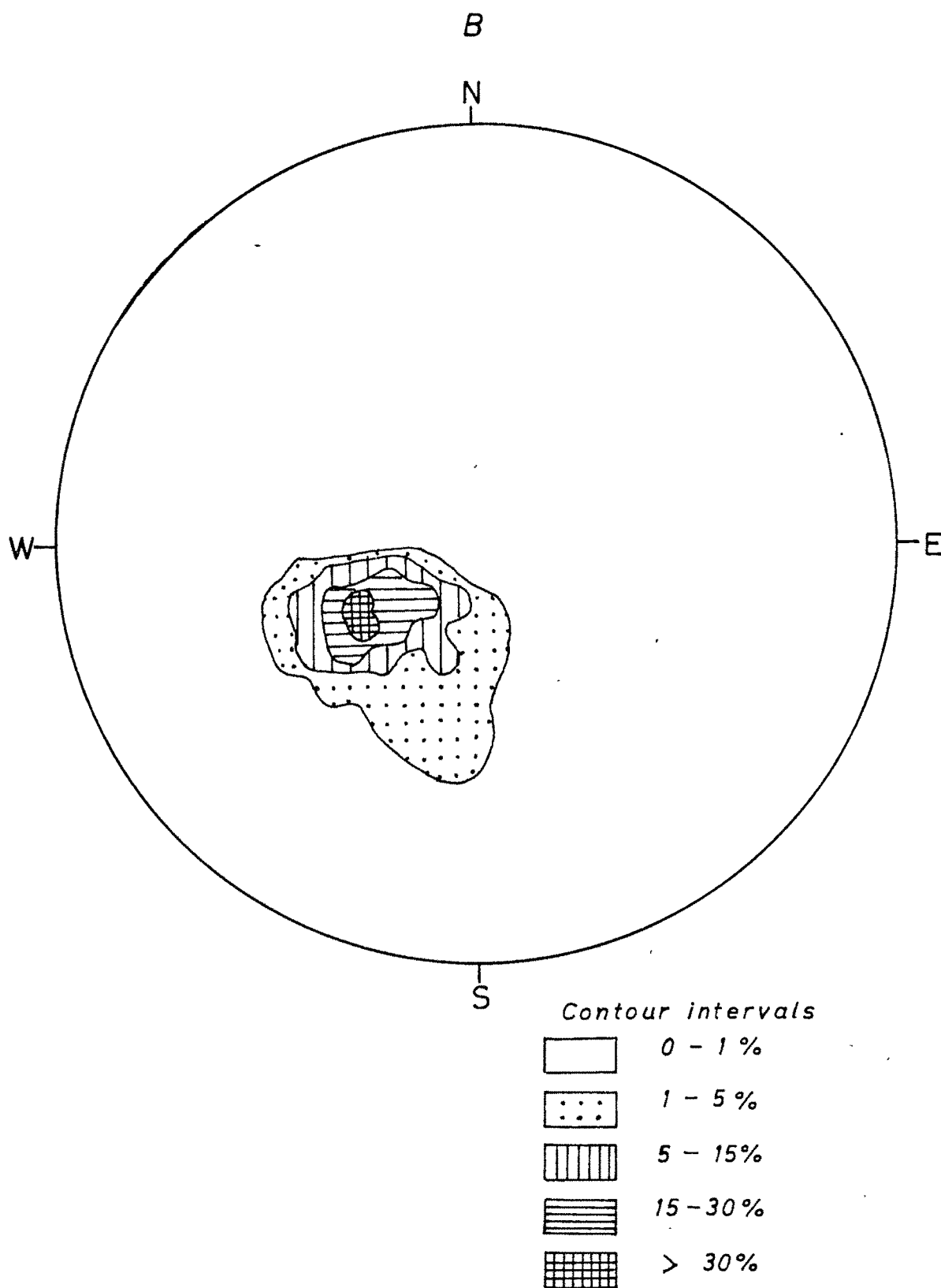
• Poles of foliation (106)

Δ L<sub>1</sub> Lineations (5)

x L<sub>2</sub> Lineations (39)

○ L<sub>3</sub> Lineations (35)

structural elements of the sub-area 10.





easterly (N68°E to S70°E) plunge. The  $L_3$  lineations show variation in plunge direction from N22°E to N44°E (Fig.IV.14A-B).

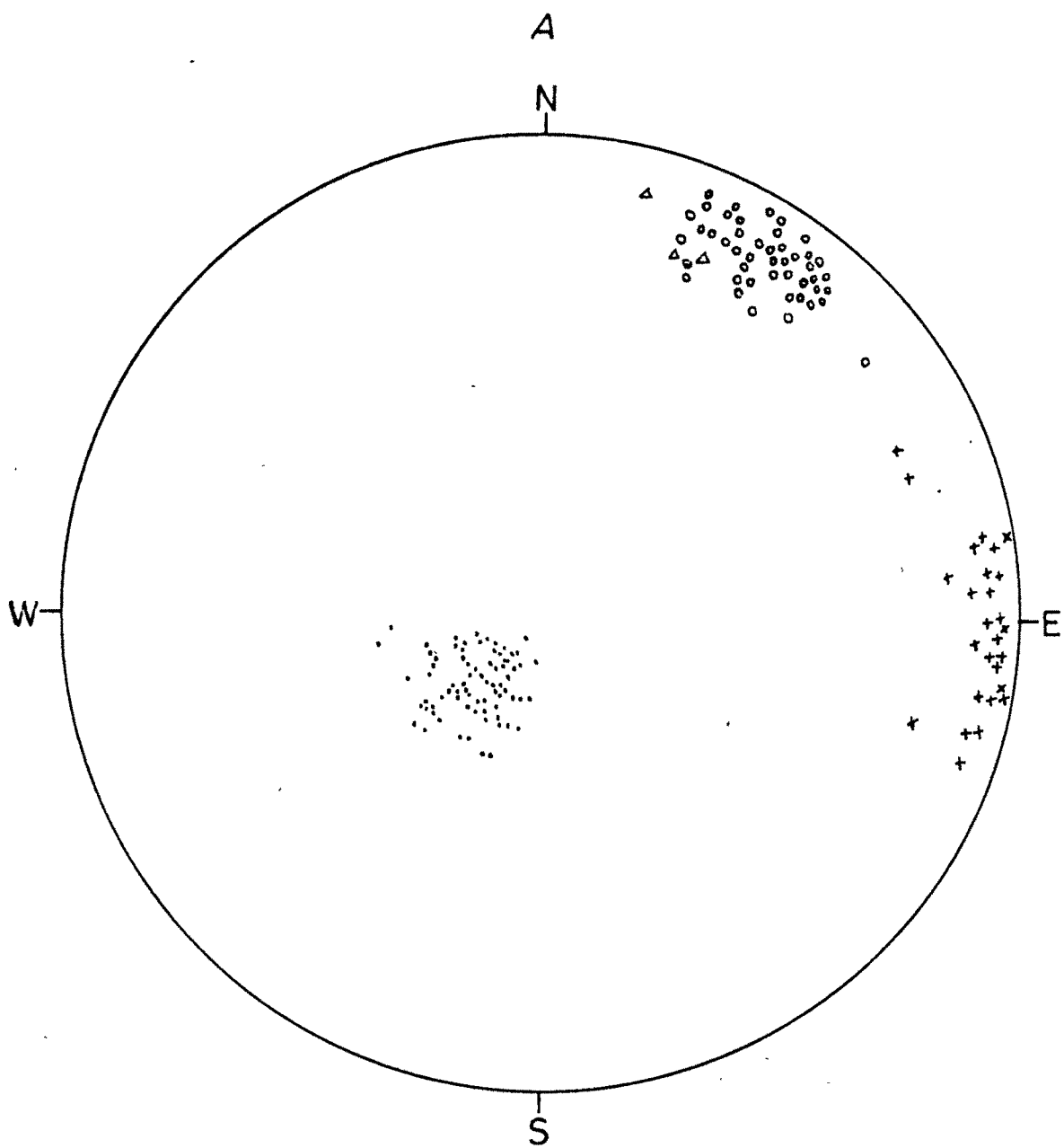
#### Sub-area (12)

This sub-area contains a small domain showing macroscopic folding on  $F_2$ . It lies to the west of sub-area (7), and its rocks consist of quartzites and garnet mica-schists. It ideally shows the folding of a quartzite band on  $F_2$  in the map. The schists too show much variation in their directions and amounts of dips due to this folding. Countoured  $\pi$ -diagram of this sub-area shows a pattern indicating two fragmentary girdles related to  $F_1$  and  $F_3$ . The  $L_1$  shows very gentle northerly plunge (N20°W to N5°E).  $L_2$  shows a scattering between E and N65°E with very low plunge.  $L_3$  - as usual in this part, plunges moderately to gently in NNE to NE (N10°E to N48°E) (Fig.IV.15A-B).

#### Sub-area (13)

Lying to the south of sub-area (6) and north of sub-area (12), this includes a relatively smaller area of quartzites and garnet mica-schists. The foliation strikes generally NW-SE with dips due NE, though flexures

## *Stereograms showing the*



• *Poles of foliation (78)*

Δ *L<sub>1</sub> Lineations (3)*

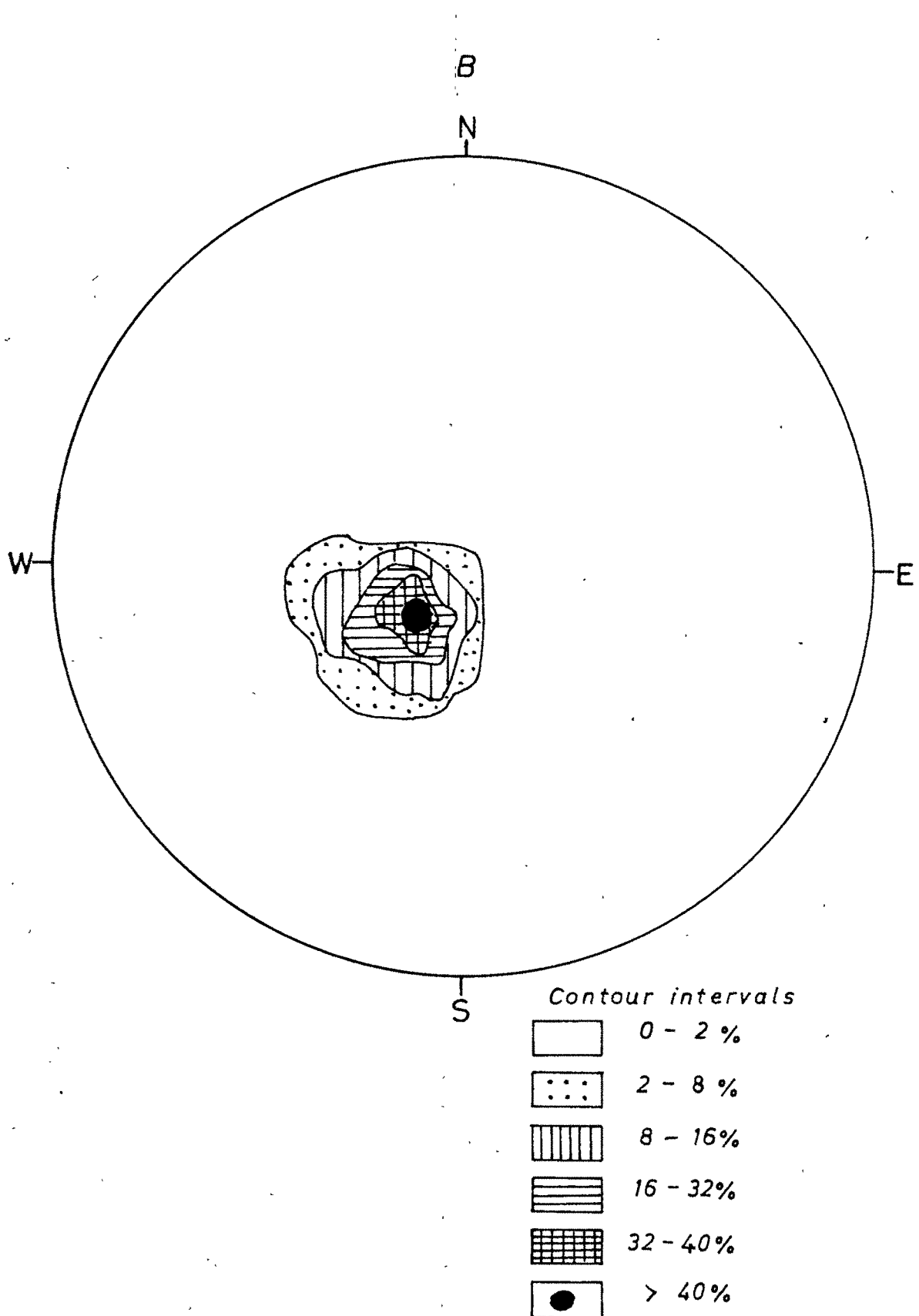
x *L<sub>2</sub> Lineations (27)*

o *L<sub>3</sub> Lineations (45)*

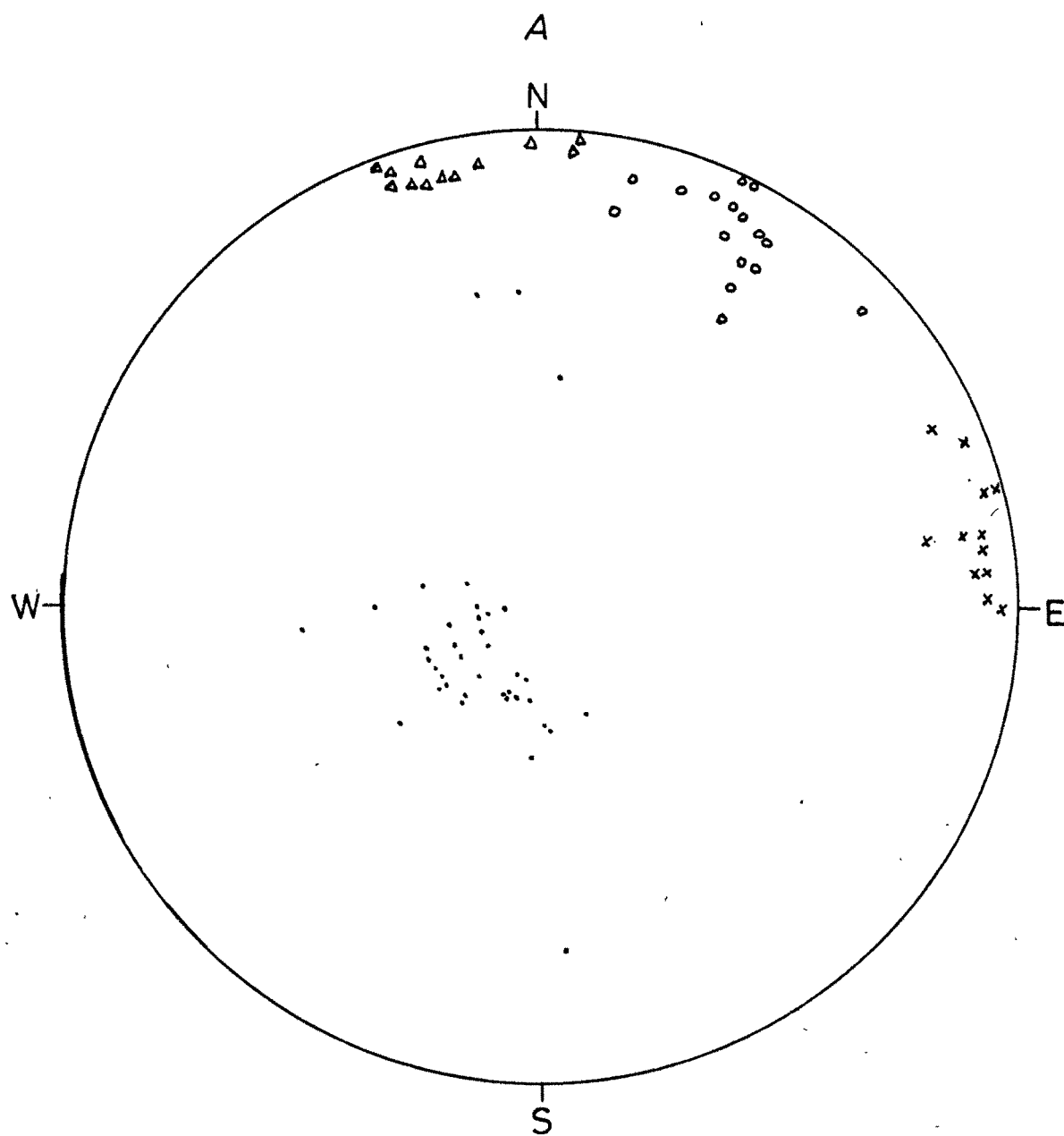
Fig. IV. 14.

structural elements of the sub-area 11.

97

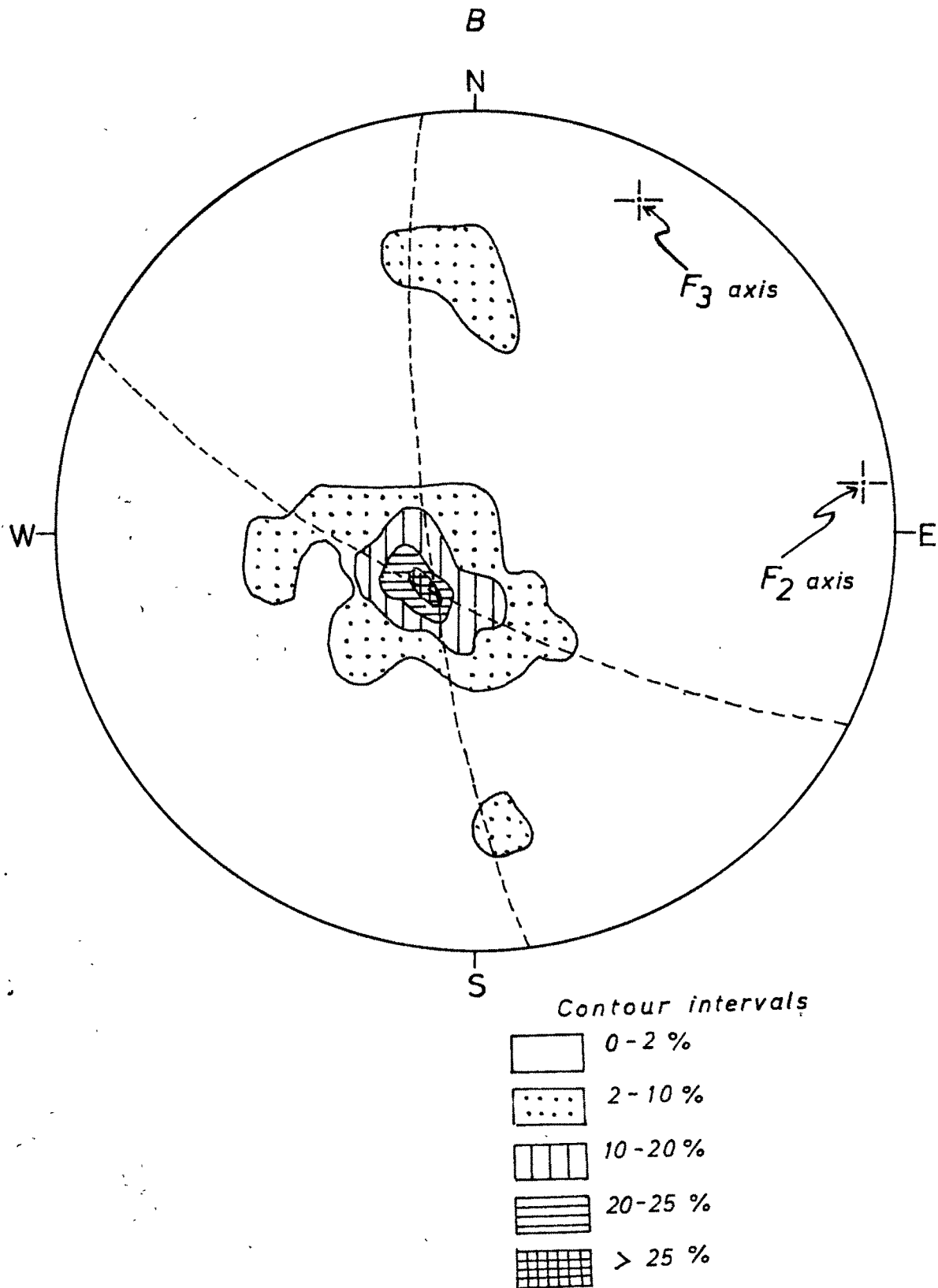


# *Stereograms showing the struct*



- Poles of foliation (38)
- Δ  $L_1$  Lineations (12)
- x  $L_2$  Lineations (12)
- o  $L_3$  Lineations (16)

ural elements of the sub-area 12.



on  $F_3$  have imparted considerable variation in the northern part of this sub-area. The  $\pi$ -diagram reveals a tendency for a girdle whose pole characterises the  $F_3$  axis. Lineations belonging to all the three generations are well developed, and show the same geometry as that in the sub-area (12) (Fig.IV.16A-B).

#### Sub-area (14)

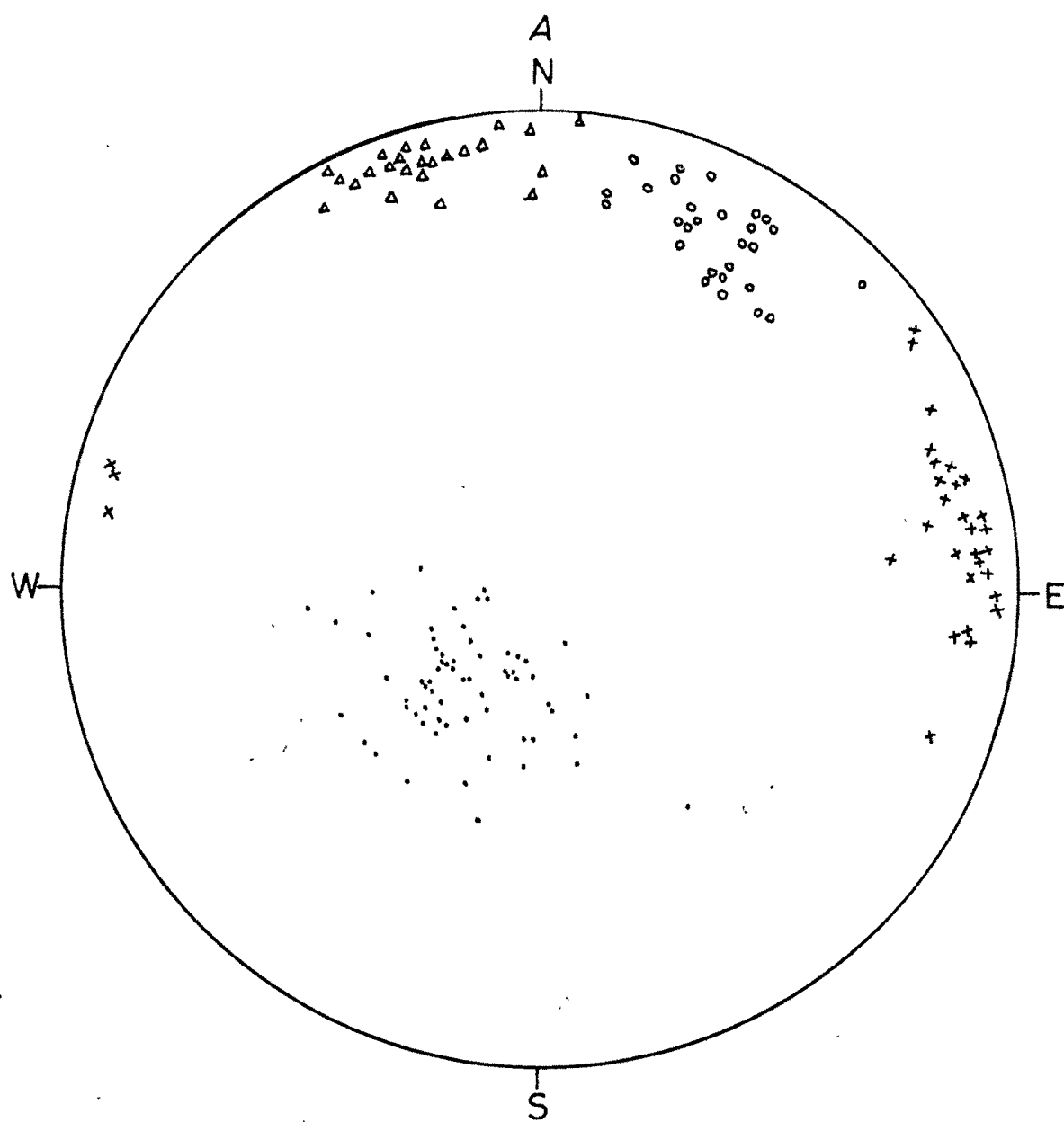
To the SW of sub-areas (12) and (13), this sub-area, comprises the eastern limb of the Matela antiform of  $F_3$  generation. The rocks are garnet mica-schists and quartzites, and the outcrop pattern of quartzites show repeated <sup>and</sup> almost reclined  $F_1$  folds on a macroscopic scale.

-diagram reveals a point maxima and obviously indicates a straight limb of the antiform without any subsidiary flexures. Lineations, however, of all the three generations are present.  $L_1$  plunges very gently due  $N5^\circ E$  to  $N24^\circ E$ .  $L_2$  is almost sub-horizontal or plunges very gently due  $N65^\circ E$  to  $S70^\circ E$ .  $L_3$  also shows very gentle plunge in directions between  $N25^\circ E$  and  $N48^\circ E$  (Fig.IV.17A-B).

#### Sub-area (15)

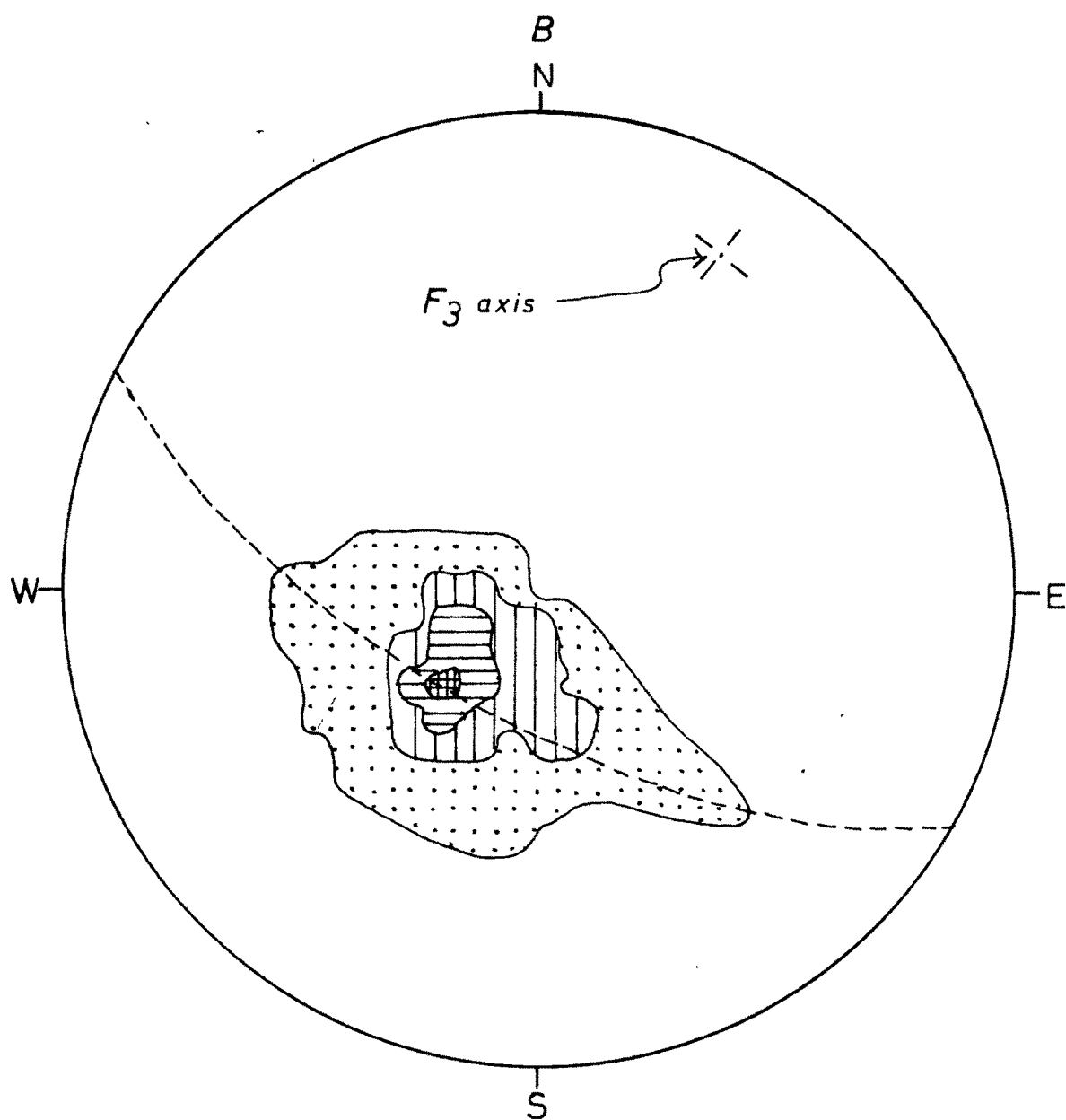
Lying to the west of sub-area (14), this includes the north-west dipping limb of the Matela antiform. The rocks, as usual are garnet mica-schists and quartzites,

## *Stereograms showing the str*


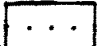





- Poles of foliation ( 65 )
- △ L<sub>1</sub> Lineations ( 23 )
- + L<sub>2</sub> Lineations ( 31 )
- L<sub>3</sub> Lineations ( 28 )

uctural elements of the sub area 13.

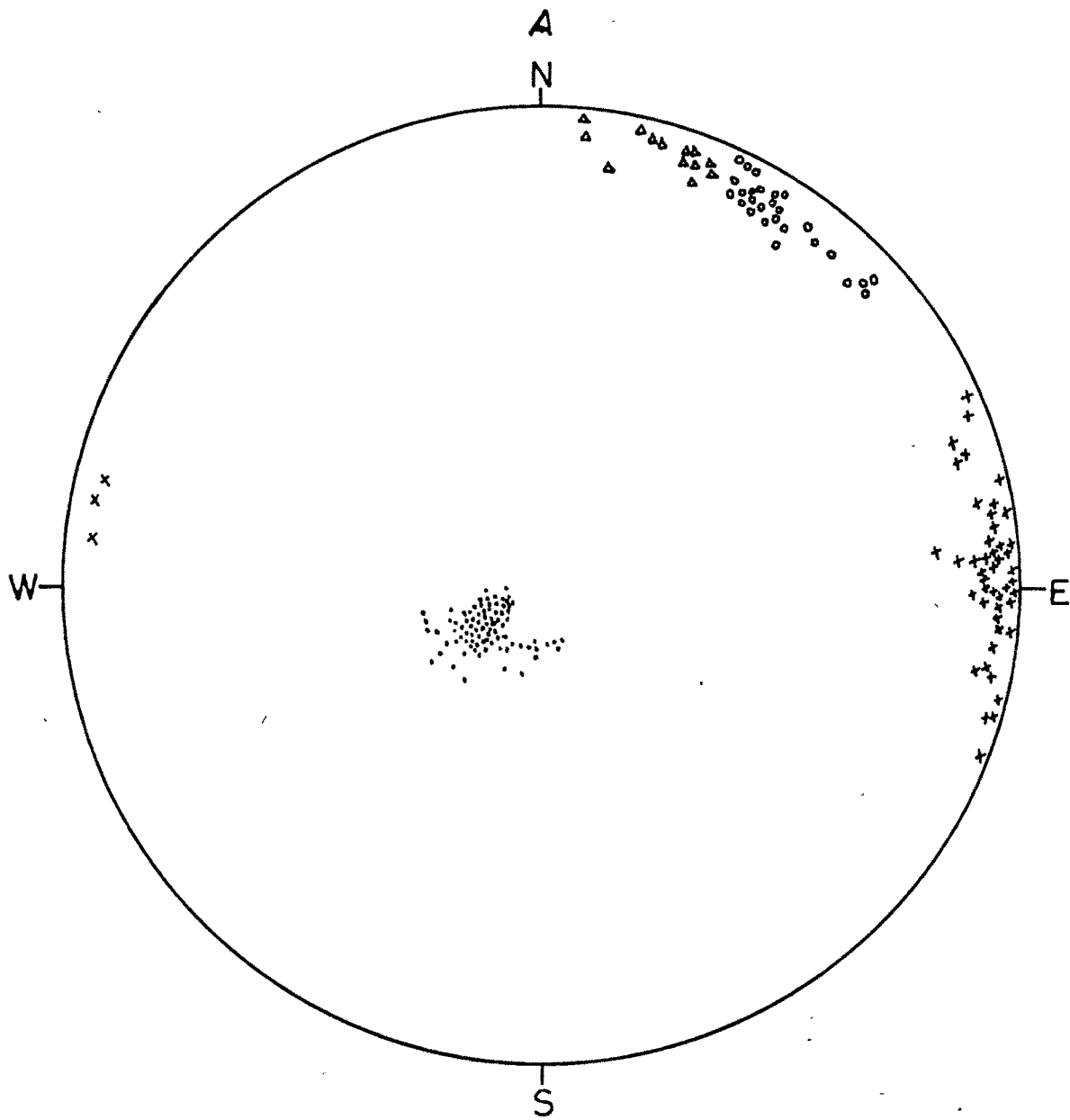


Contour intervals:-

	0 - 1 %
	1 - 10 %
	10 - 25 %
	25 - 45 %
	> 45 %



## *Stereograms showing the struc*

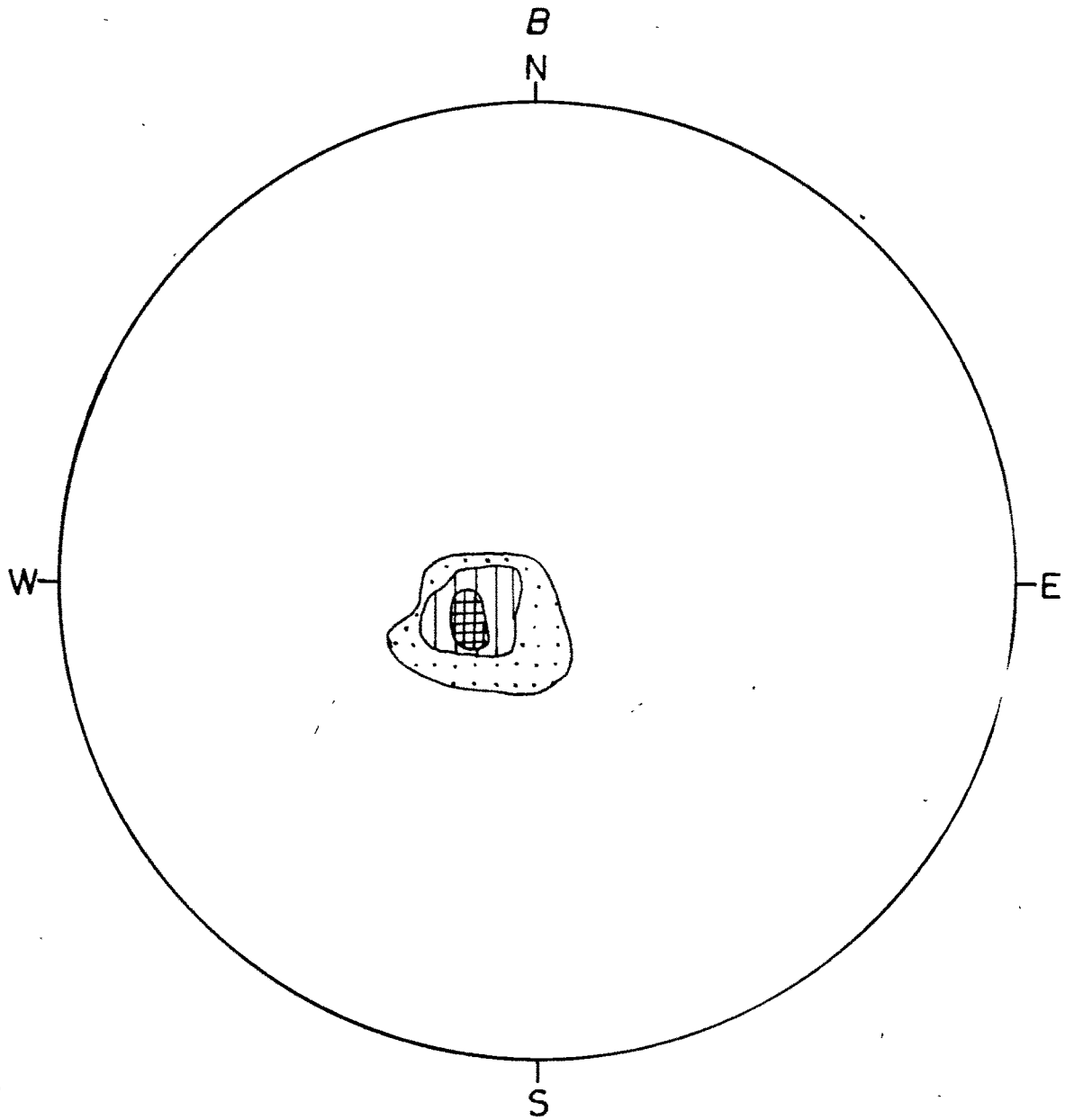


- Poles of foliation (116 )
- Δ L<sub>1</sub> Lineations (13 )
- + L<sub>2</sub> Lineations (44 )
- L<sub>3</sub> Lineations (28 )


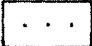


Fig. IV.17.

tural elements of the sub-area 14.

101



Contour intervals:-

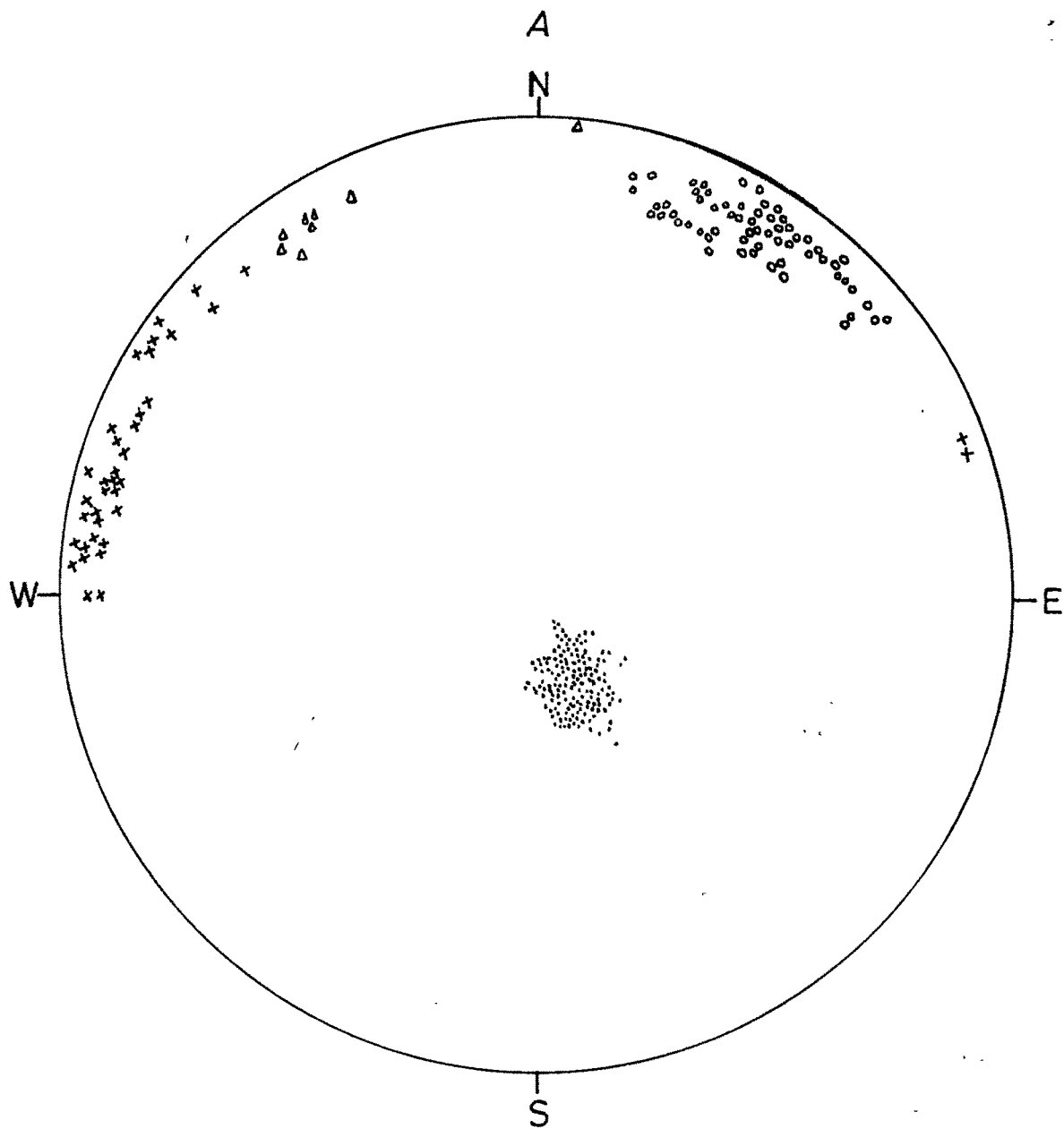
	0 - 10 %
	10 - 40 %
	40 - 70 %
	> 70 %

the quartzite forming intercalations perhaps on account of  $F_1$  folding. The contoured  $\pi$ -diagram reveals little. The  $L_1$  shows the usual plunge of a few degrees only in directions between N30°W to N5°E. The  $L_2$  lineation is mostly plunging in the NW quadrant, and the angle of plunge is very low - a few degree only. The direction of plunge has a wide range from N40°W to W and as much as N70°E.  $L_3$  is quite prominently developed, and has the general trend and plunge varying between N15°E and N50°E (Fig.IV.18A-B).

#### Sub-area (16)

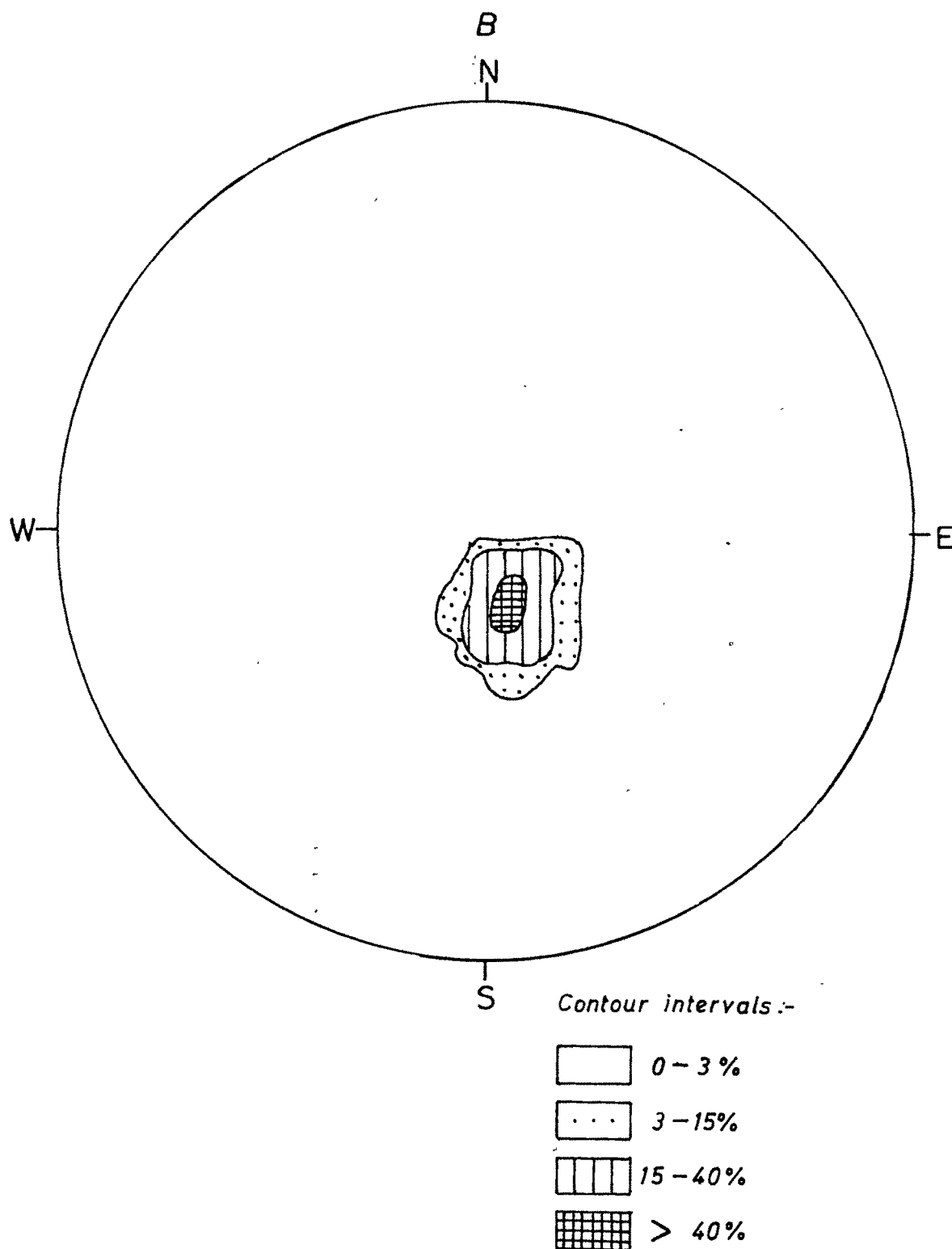
This sub-area, to the immediate SW of sub-area (14), has almost identical structural geology. The rocks are garnet mica-schists, quartzites and tourmaline gneiss. The foliation has an overall strike of WNW-ESE, with moderate dip due NNE.  $L_1$  is represented only feebly by a few readings and in all cases, it plunges gently due N5°E to N12°E.  $L_2$  is almost horizontal, with only a plunge of 5° to 10° in directions varying between N78°E and S65°E and W.  $L_3$  is quite prominent, shows gentle plunge, the direction varying from N28°E to N50°E (Fig.IV.19A-B).

## Stereograms showing the str

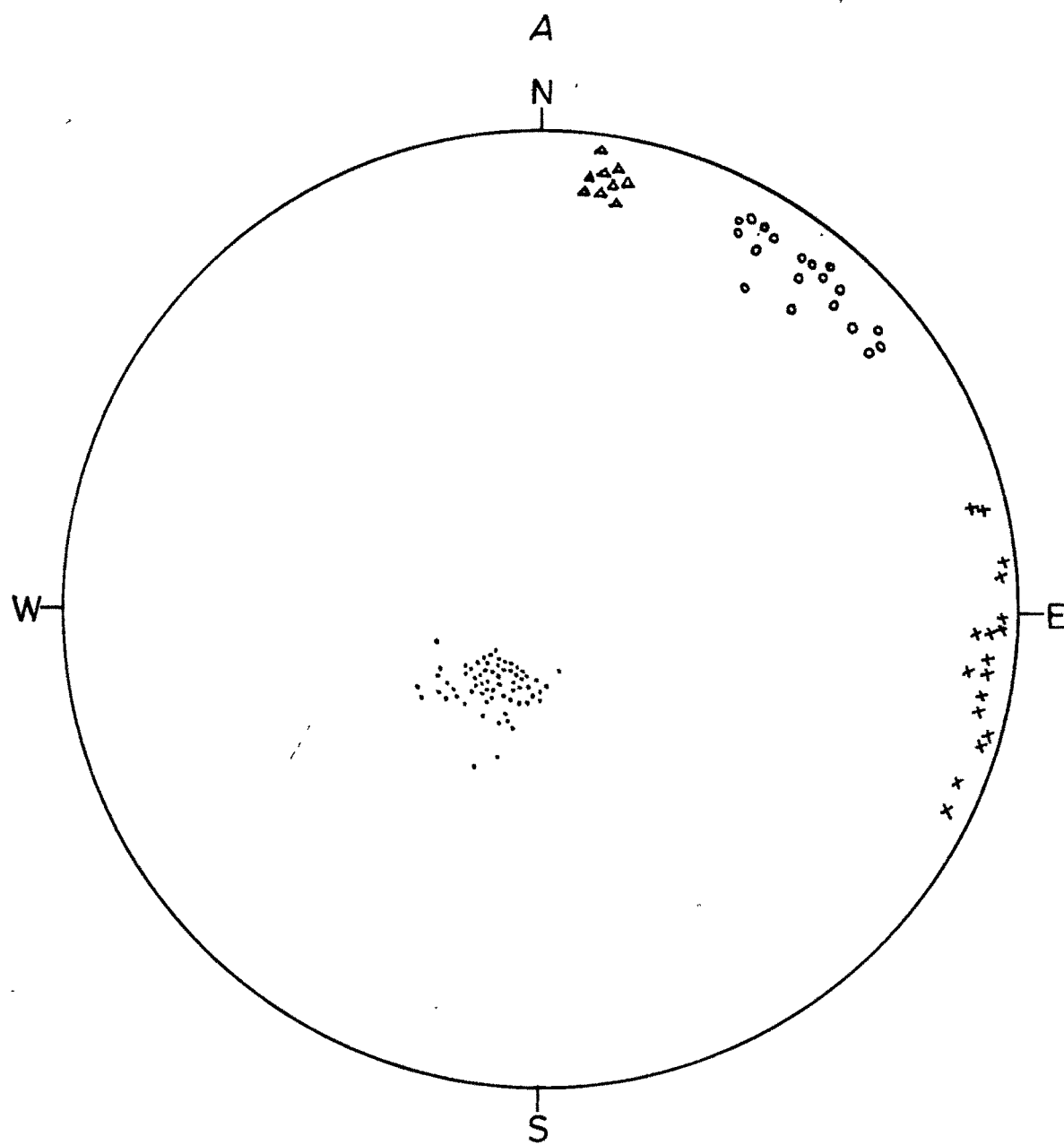


- Poles of foliation (197)
- △  $L_1$  lineations (8)
- x  $L_2$  lineations (37)
- $L_3$  lineations (61)

Structural elements of the sub-area 15.

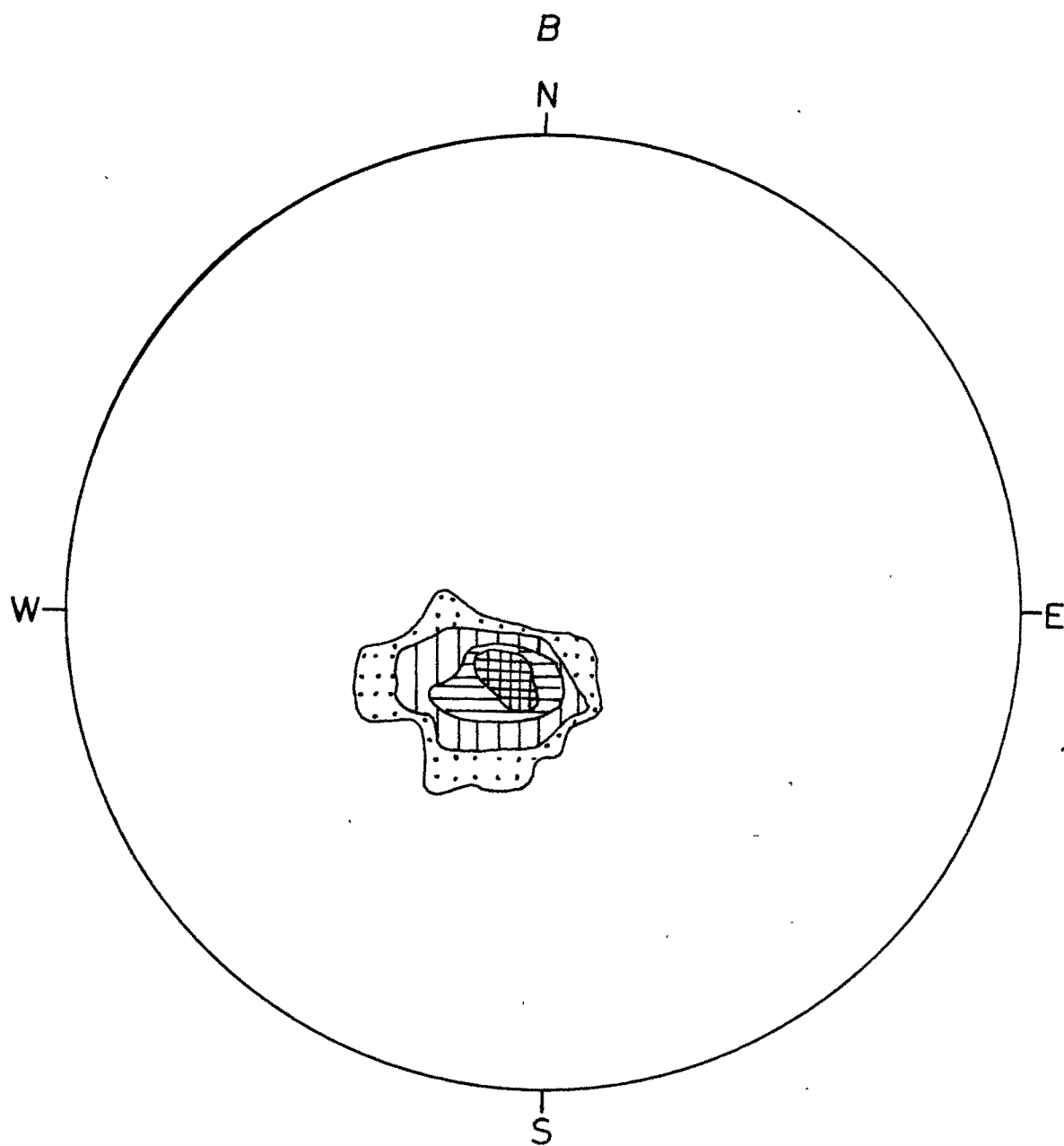


# *Stereograms showing the st*


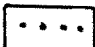
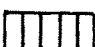
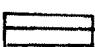
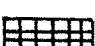


- Poles of foliation (65)
- Δ  $L_1$  Lineations (9)
- x  $L_2$  Lineations (17)
- $L_3$  Lineations (19)

structural elements of the sub-area 16.



Contour intervals

	0 - 2 %
	2 - 10 %
	10 - 40 %
	40 - 90 %
	> 90 %

Sub-area (17)

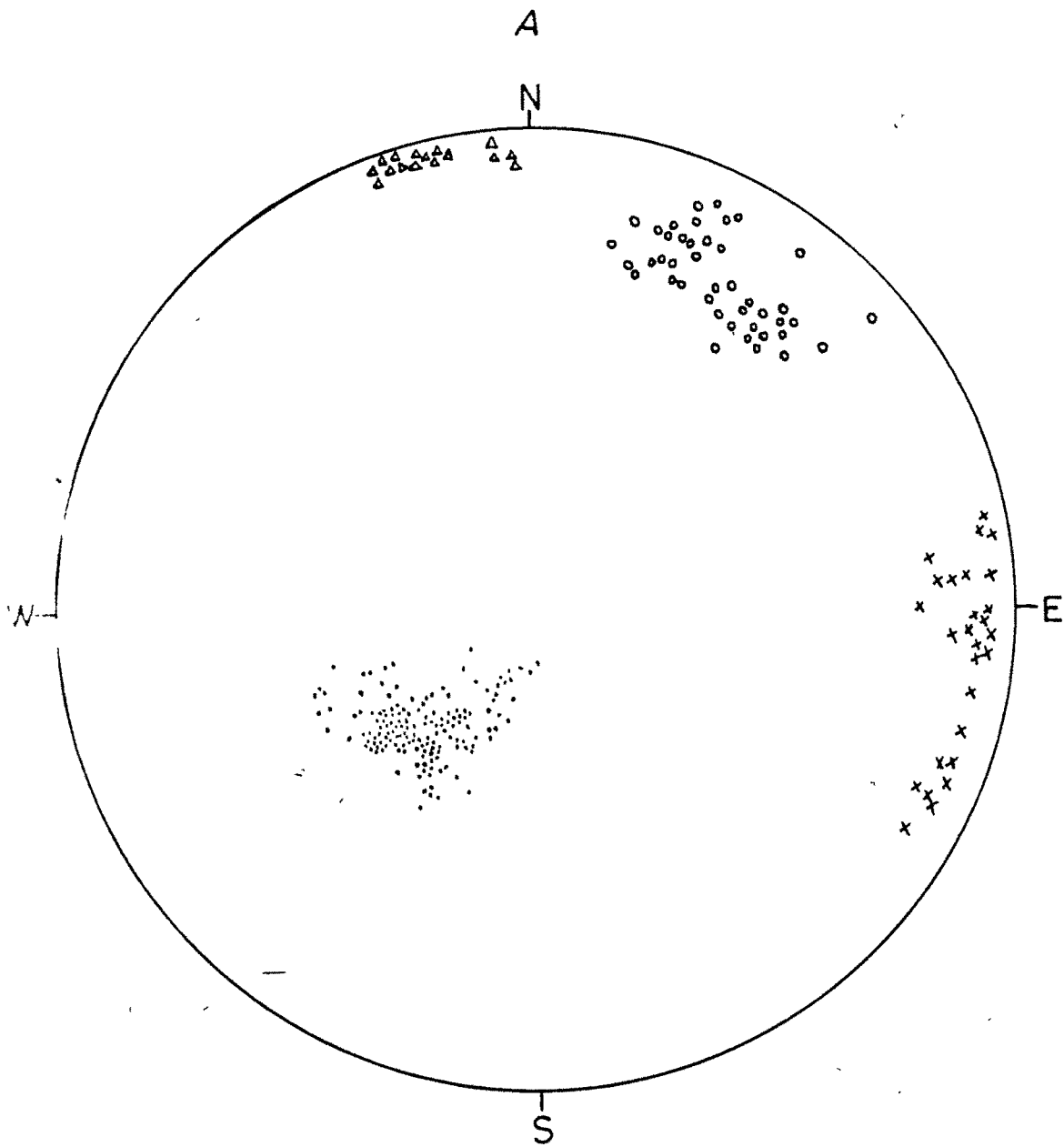
Occupying the SW corner of the map, this sub-area lies to the south of sub-area (16). The rocks are gneissic granites, gneisses, mica-schists and quartzites. The foliation is seen striking NW-SE, dipping moderately due NE. No macroscopic folds are clearly recorded. But it appears that the main Dyolidanda hill of the gneissic granites perhaps comprises an obliterated early  $F_1$  fold. Quartzite bands too perhaps indicate a  $F_1$  reclined fold. The effects of  $F_2$  and  $F_3$  are seen only as linear structures.  $L_1$  is seen plunging very gently in direction varying between N and  $N20^\circ W$ .  $L_2$  has an easterly plunge from  $N80^\circ E$  to  $S60^\circ E$ .  $L_3$  is most prominent and widely developed. It shows gentle to moderate plunge in the directions ranging from  $N12^\circ E$  to  $N50^\circ E$ .  $\pi$ -diagram reveals little of the fold pattern (Fig.IV.20A-B).

Sub-area (18)

This sub-area, comprising the south-western corner of the map, is structurally identical to sub-area (17), and in all respects, has the same structural characters as the latter (Fig.IV.21A-B).



## *Stereograms showing the st*

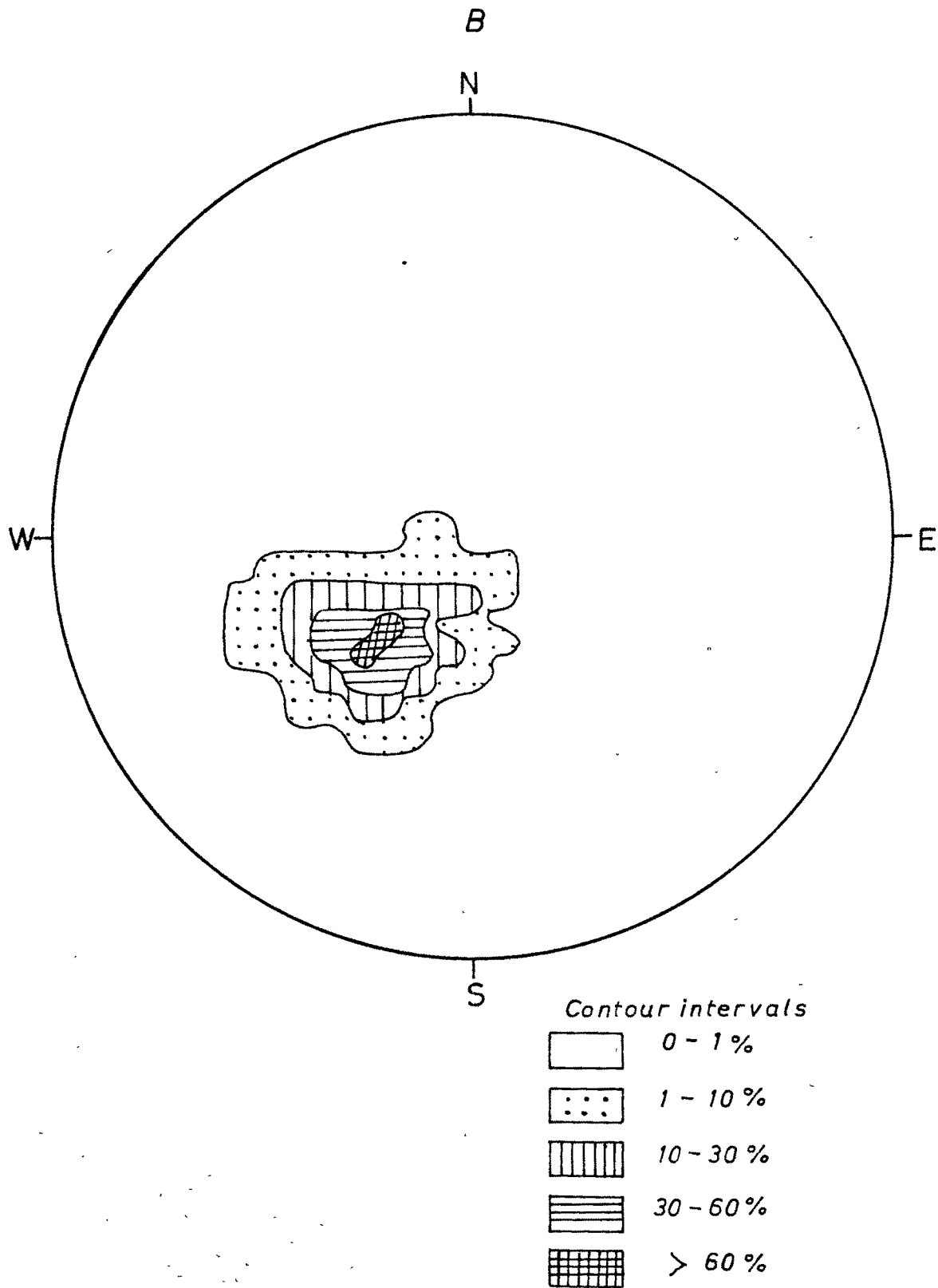


- Poles of foliation (120)
- Δ  $L_1$  Lineations (16)
- x  $L_2$  Lineations (28)
- $L_3$  Lineations (43)

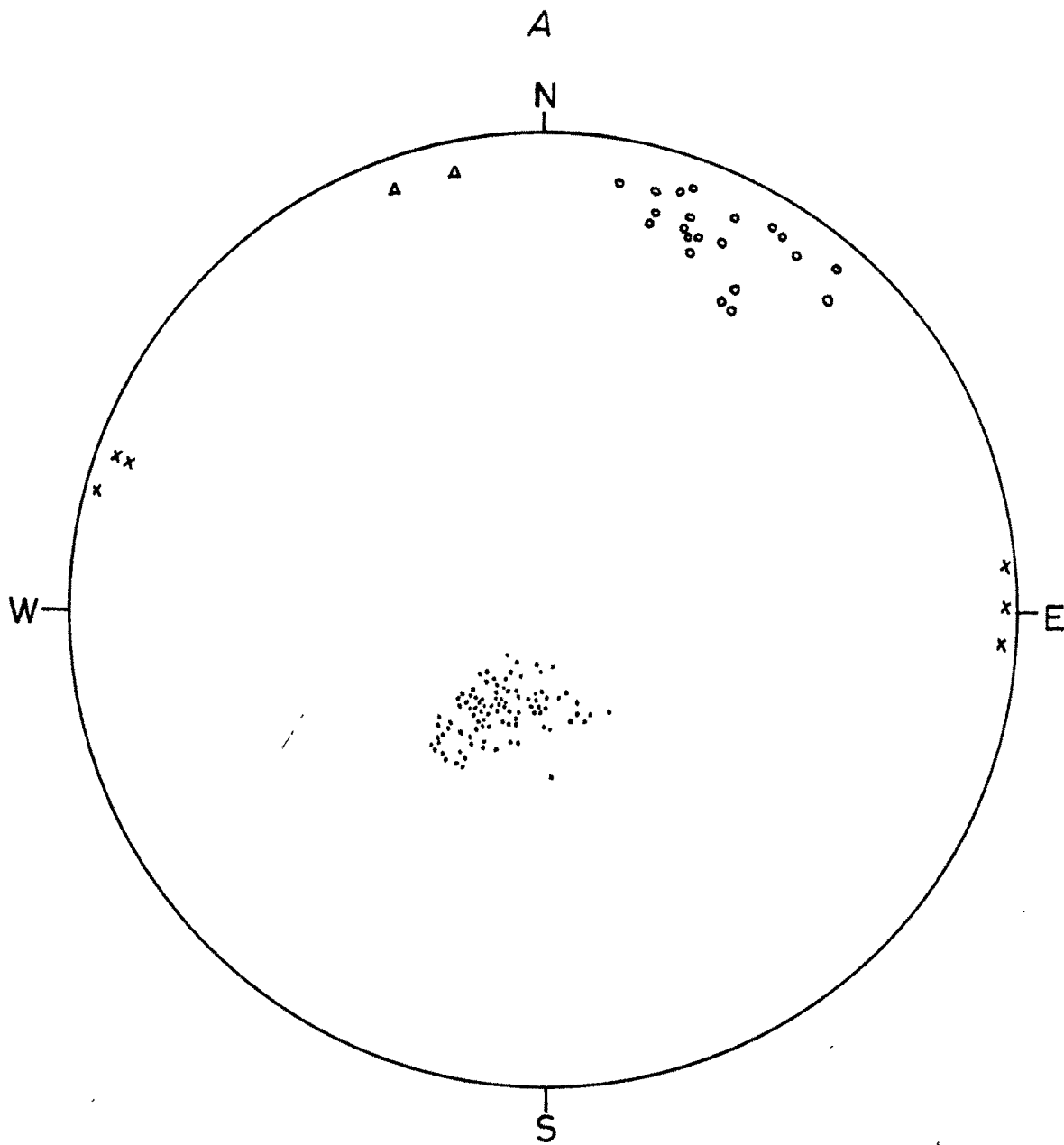
Fig. IV. 20.

Structural elements of the sub-area 17.

106

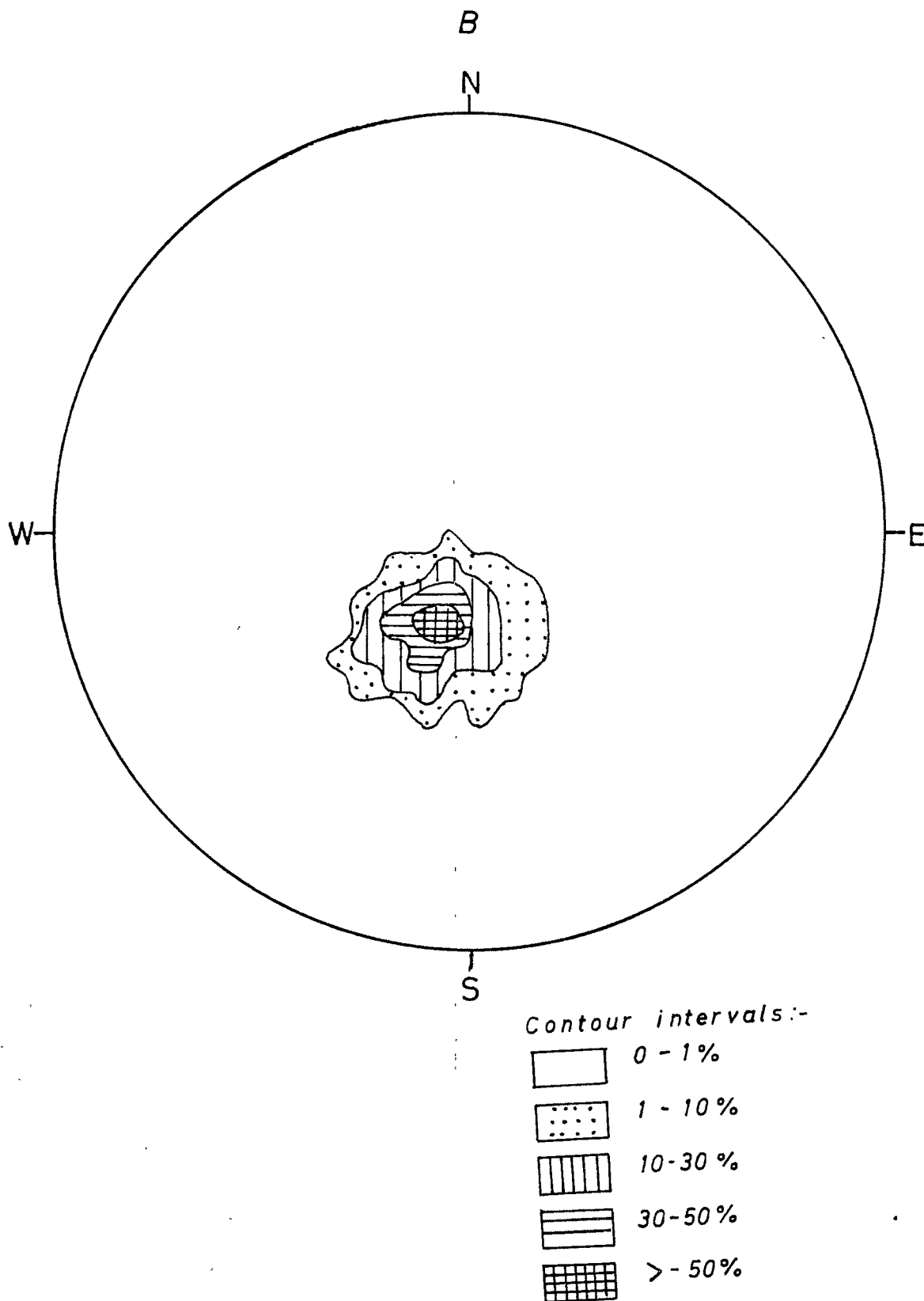


# *Stereograms showing the structure*



- Poles of foliation (88)
- Δ L<sub>1</sub> Lineations (2)
- x L<sub>2</sub> Lineations (6)
- L<sub>3</sub> Lineations (21)

iral elements of the sub - area 18.



## STRUCTURAL SYNTHESIS

A synthesis of the information furnished by the various sub-areas, reveals an interesting structural pattern - a pattern that has originated as a result of the interference of at least three major fold events. Each fold event has not only left its mark on a regional scale, but minor structures related to it, with their characteristic styles and orientation, provide a very valuable tool in recognising the effects of the particular folding. The author's analysis of the area has fully substantiated the findings of the early workers like Merh (1968), Merh and Vashi (1965), Desai (1968) that the Almora nappe has undergone three main foldings.

In Almora area, the effects of all the three fold episodes are recognised both at macroscopic and mesoscopic scales. The outcrop pattern typically reveals interference of  $F_1 - F_2$ ,  $F_1 - F_3$  and  $F_2 - F_3$  in different parts of the area. The author has in the following pages of this chapter, given a brief account of the folds of various generations and their mutual interference.

### Nature of the first folding ( $F_1$ )

This folding shows widespread effect and is typically revealed by the quartzites. Tight reclined

folds of this generation are easily recognised on the map by the shapes of the quartzite outcrops. The repeated occurrence of long narrow and lensoid quartzite layers in schists is obviously due to the repeated folding of only a few quartzite layers, such that at most places the fold hinges have broken and the limbs stretched and boudinaged as detached lenses.  $F_1$  folds of all dimensions ranging from several meters to a few centimeters in length, preserved in quartzites are recorded in almost all parts of the area. The main schistosity ( $S_1$ ) which shows axial plane relationship with the folds, is related to  $F_1$  folding. This schistosity, as the author has found out, is not the primary one having developed directly from the sediments during  $F_1$  as envisaged by Merh and Vashi (1965), but is derived by the tight microfolding of an earlier schistosity. At several places, folded relicts of the earlier schistosity ( $S$ ) has been recorded, viz., in sub-areas (17), (5) and (6). The various linear structures  $L_1$ , related to  $F_1$ , have already been described earlier. It is interesting to find that the orientations of  $S_1$  and  $L_1$  have been considerably modified by the effects of later folding  $F_2$  and  $F_3$ .

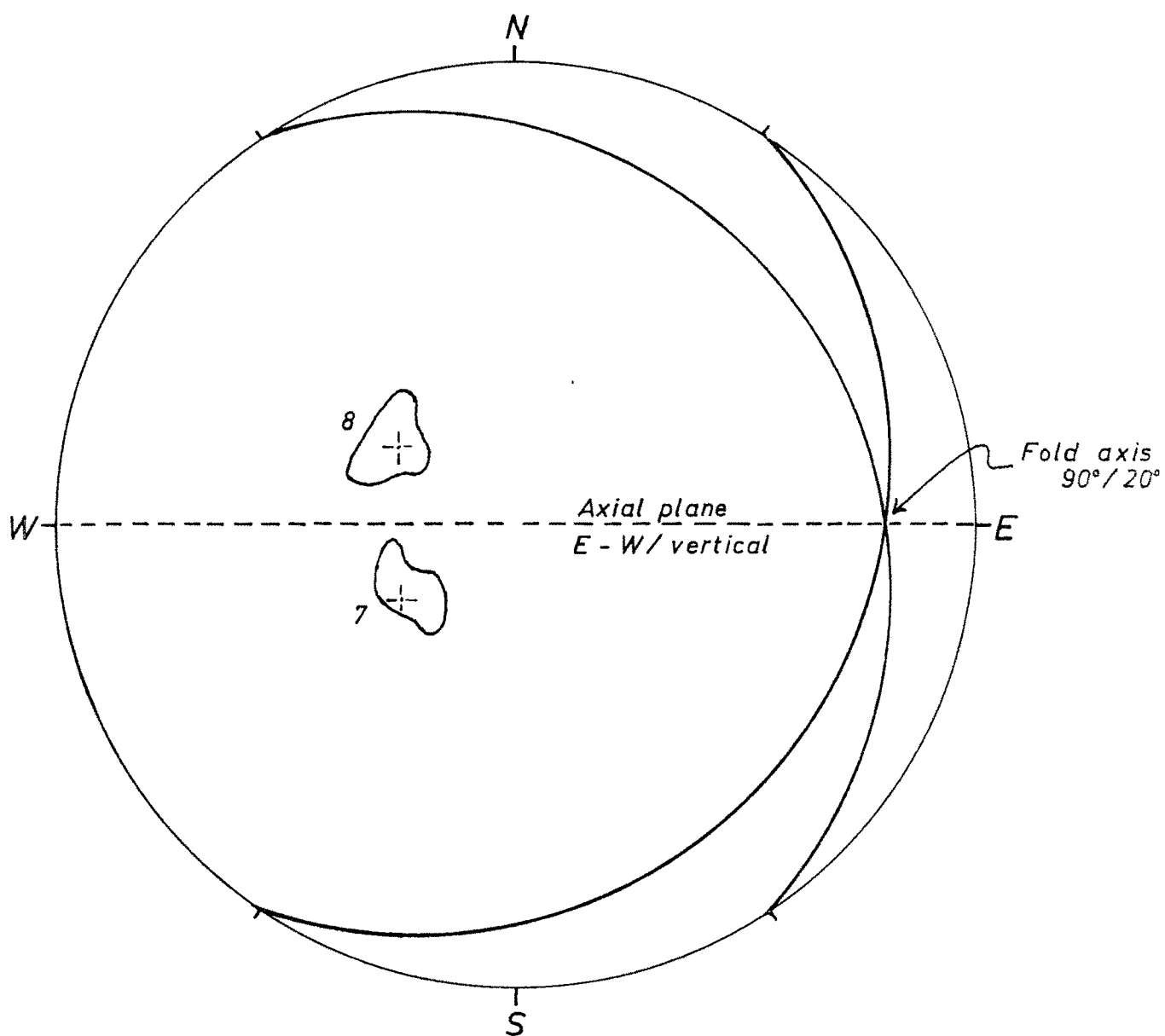
### Nature of the second folding ( $F_2$ )

The second fold episode ( $F_2$ ) was responsible for the development of the large Almora nappe synform. During this folding, in addition to the formation of the main synformal structure, a number of smaller macroscopic folds developed on the two flanks of the main fold. The study area, that lies mostly on the southern flank of the synform, contains smaller antiforms and synforms of  $F_2$  generation. A very small portion of the main synformal hinge falls within the study area, in the extreme NE, comprising the sub-areas (1) to (5). This structure has been referred to as Dinapani-Kaparkhan synform, and its hinge has a ENE-WSW strike, with an axial plunge of a few degrees due east. On account of the effects of the superimposition of  $F_3$  flexures, this synformal structure has been rendered quite irregular and distorted.

Along the eastern part of the area, the Sual antiform and its complimentary Guna synform, comprise two macroscopic structures of  $F_2$  origin. The Sual antiform ideally shows its superimposition over  $F_1$  folds. The two structures mainly lie within the sub-areas (7), (8) and (9). The fold axis of this antiform calculated from the collective  $\beta$ -diagram (Fig.IV.22) of sub-areas (7)

Fig. IV. 22.

*Collective  $\beta$  diagram of sub-areas 7 and 8.*





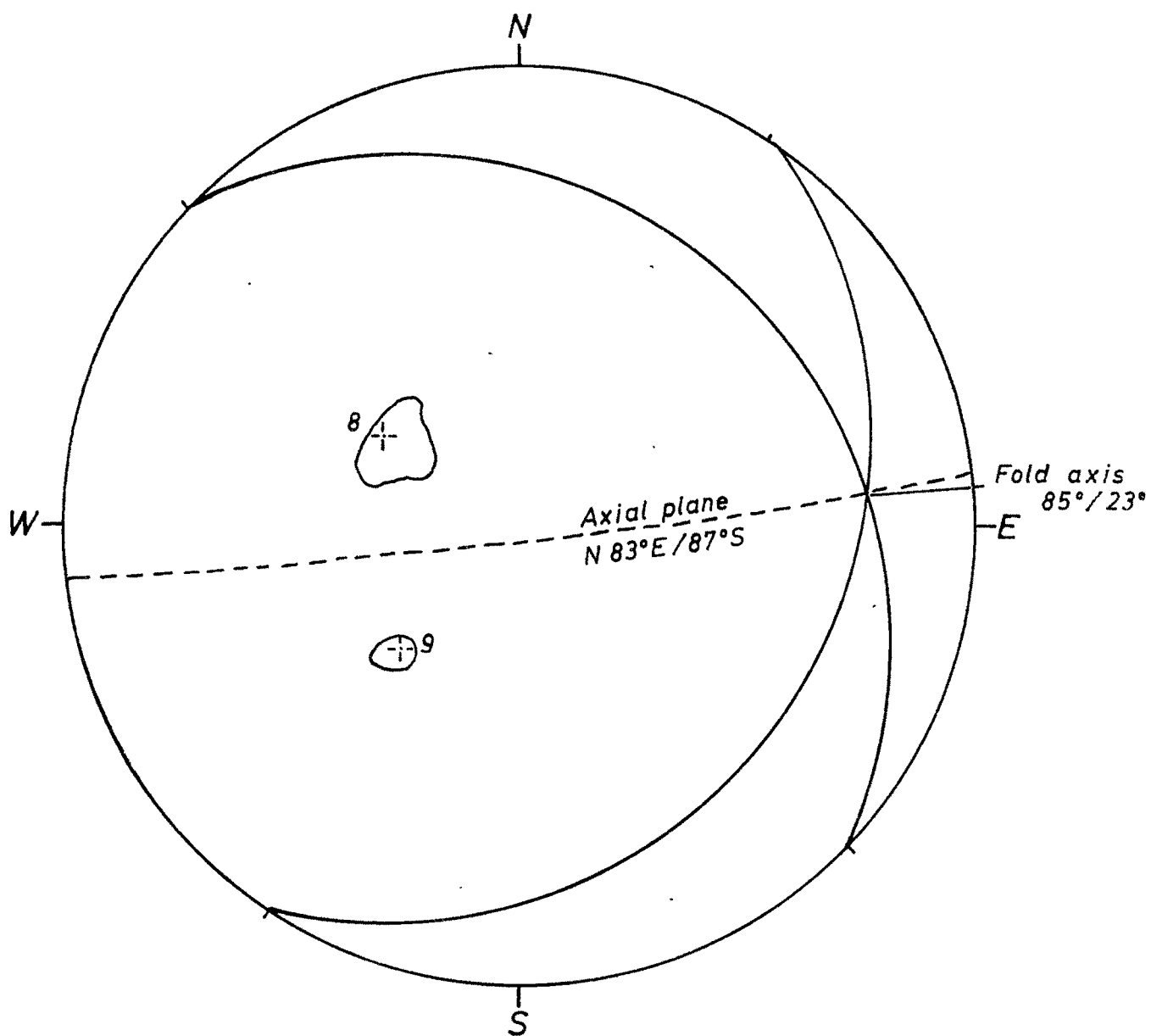
and (8) shows a plunge of  $20^\circ$  in the east direction, and the axial plane strikes E-W and is almost vertical. The Guna synform to the south, has almost a similar geometry, the axial plunge being  $23^\circ$  due  $N85^\circ E$ , and the axial-plane dipping  $87^\circ$  due  $S$  as shown by the collective  $\beta$ -diagram (Fig.IV.23 of sub-area (8) and (9)).

This  $F_2$  folding has resulted into widespread crinkling and microfolding of the schistosity. The axes of these tiny folds (generally forming puckers) show gentle to moderate plunge - either westward or eastward - the latter direction being more common. An interesting feature of this  $L_2$  lineation is that its direction of plunge fluctuates considerably - the range of fluctuation being between ENE to SE and WNW to WSW (Fig.IV.24). The author is of the opinion that the scattering of the  $L_2$  plunge direction is due to a combination of following reasons:-

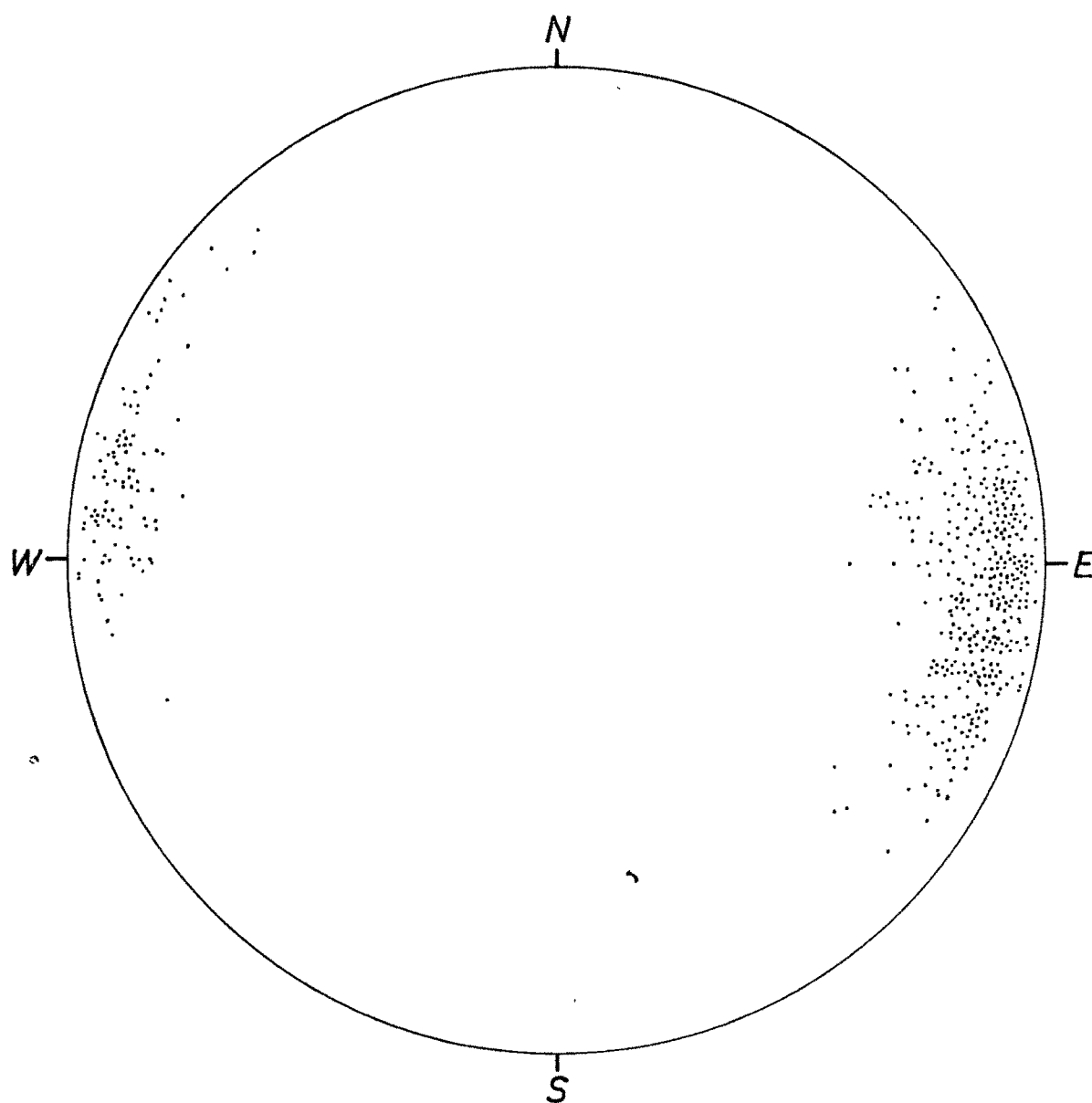
- (1) Variation in the strike and dip of the axial planes. The strike is seen to vary between ENE-WSW and SE-NW. Some variation is obviously due to the effect of  $F_3$ , but it is most likely that the axial-plane of the microfolds even originally showed strike variation. Similarly, the variation in the dips of the axial-planes have also

Fig. IV.23.

Collective  $\beta$  diagram of sub-areas 8 and 9.



*Stereogram showing scattering of  $L_2$  lineations.*



• *Lineations (482)*

contributed to the change in the fold axis ( $L_2$ ) trends. It has been observed that the axial-planes of  $F_2$  microfolds and the associated strain-slip cleavage ( $S_2$ ) are either vertical or dip steeply due N or S.

(2) The orientation of the folded surfaces ( $S$  and  $S_1$ ).

As the  $F_2$  flexures were superimposed on a terrain comprising numerous  $F_1$  folds with a strong axial-plane ( $S_1$ ) cleavage, the superimposition of the  $F_2$  axial-planes on differently oriented surfaces -  $S$  (bedding etc.) and  $S_1$  (schistosity) has resulted into a scattering of  $L_2$  orientation.

(3) The superimposition of  $F_3$  folding. The development of  $F_3$  folds - especially the Matela antiform in the west, is obviously responsible for the increase in the plunge of  $L_2$  in the eastern part and for a westerly plunge in the western part.

Effects of  $F_2$  on  $F_1$ -

The south dipping northern limb of the Dinapani-Kaparkhan synform (sub-areas 1 and 2) does not show any significant  $F_1$  -  $F_2$  interference effect, except that the  $L_1$  is seen dipping south-westerly. Similarly in

the sub-areas (3), (4) and (5), that comprise the north dipping limb, the effects of the superimposition of  $F_2$  on  $F_1$  are recorded only in the folding of the  $L_1$ . The  $L_1$  shows a northerly plunge. Good examples of  $L_1$  being folded by  $F_2$  are encountered in sub-area (5) (Plate IV.6).

Refolding of  $F_1$  structures by  $F_2$  is ideally shown on a macroscopic scale in the sub-areas (7), (8), (12) and (13), the rocks of which comprise a large  $F_2$  antiform (Sual antiform). On the map itself the refolding of a tightly and repeatedly folded quartzite is clearly seen. The  $S_1$  (schistosity) shows extensive micro-folding and crinkling due to  $F_2$ . A crenulation cleavage  $S_2$  is thus superimposed over  $S_1$ .

The  $L_1$  lineation also has been affected. In the sub-areas (7), (12) and (13), that comprise the northern limb of the Sual antiform,  $L_1$  shows a northerly plunge, while on the southern limb in the sub-area (8), it plunges southwesterly.

#### Nature of the third folding ( $F_3$ )

This folding has given rise to a large antiform (Matela antiform) in the western half of the study area. Smaller macroscopic folds of this generation have also developed on the north dipping limb of the Dinapani-Kaparkhan ( $F_2$ ) synform. The Matela antiform is an open

PLATE IV.6

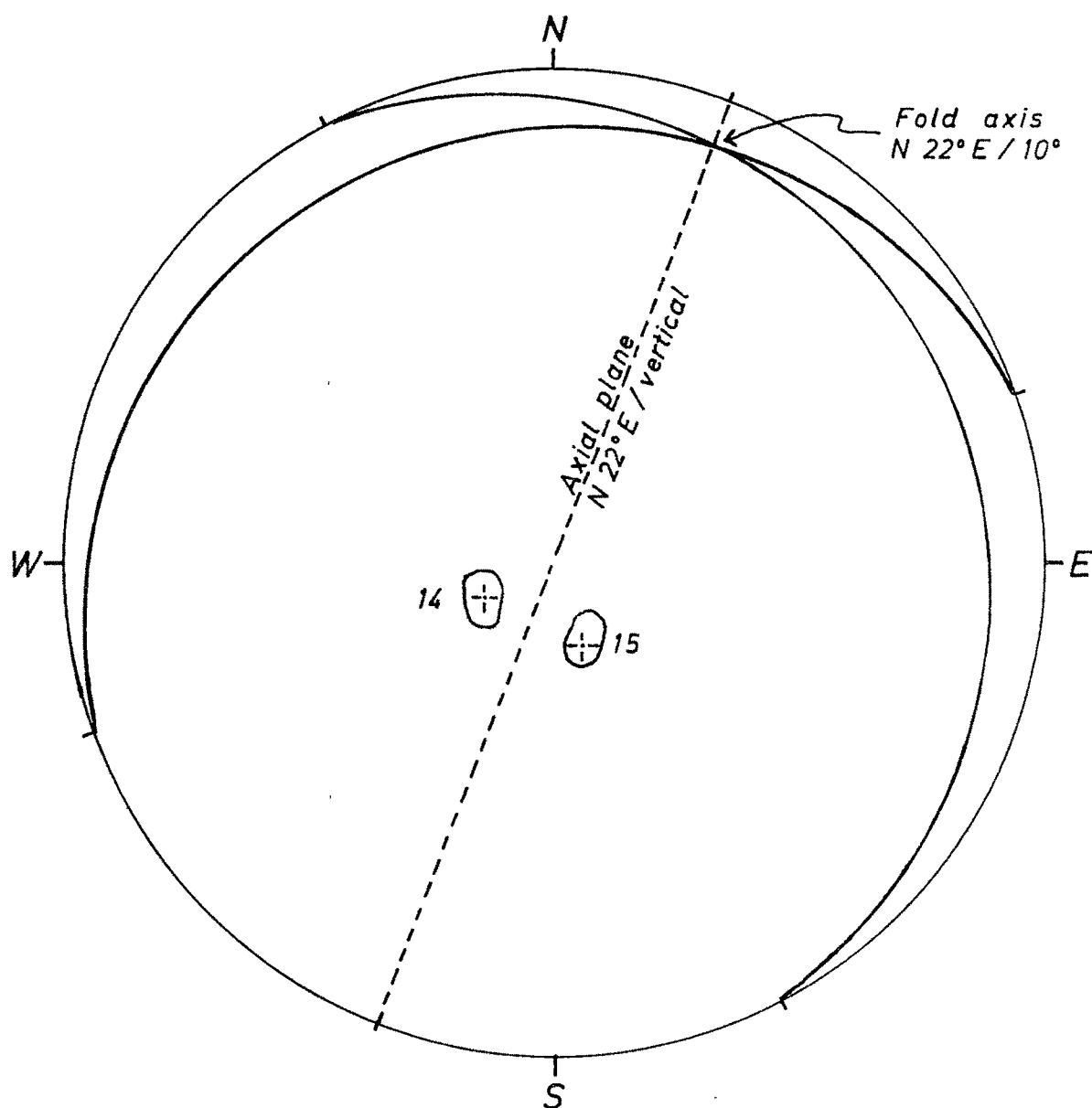
$L_1$  lineation of ribbon type folded on  
 $F_2$  (Loc. south of Kasardevi)

arch like structure, whose western limb lies within the sub-area (15) and the eastern limb is shared by the sub-areas (14) and (16). Southward (in the sub-areas 17 and 18) this antiformal structure tends to fade out gradually. The fold axis of this antiform calculated from the  $\sigma$ -diagram (Fig.IV.25) of the average foliation trends of the sub-areas (14)<sup>and</sup> (15) ~~and (16)~~, shows a plunge of  $10^\circ$  due  $N22^\circ E$ . The mean axial-plane is almost vertical, though the actual measured axial-planes of the small  $F_3$  folds and micro-folds generally show dips of  $80^\circ$  to  $87^\circ$  due E.

The behaviour of  $F_3$  in the NE corner in sub-areas (1), (2), (3), (4) and (5) is quite interesting. While  $F_3$  folds in the sub-areas (1) and (2) are of the nature of very gentle flexures with a south dipping axis, those in the sub-areas (3), (4) and (5) are very conspicuous, rather sharp and with angular hinges. The axial-plane of these  $F_3$  folds, that can be recognized clearly on the map even, (Fig.IV.3), are almost NE-SW trending in the sub-area (3), while it swings to almost NS in the sub-area (5). This swing in the trend of the axial-planes appears to be an original feature of the  $F_3$  folding.

Fig. IV. 25.

Collective  $\beta$  diagram of sub-areas 14 and 15.





### Effects of $F_3$ on $F_1$ —

On a regional scale, the  $F_3$  antiform (Matela antiform) is seen refolding a group of  $F_1$  folds. This is quite evident from the outcrop pattern and the trend of the quartzite bands in sub-areas (14), (15) and (16). In sub-area (6), too, a relatively small macroscopic  $F_3$  fold is seen developed on one of the limbs of a big  $F_1$  fold.

So far as the effects of  $F_3$  on  $S_1$  and  $L_1$  are concerned, they are recognised all over the area. The  $S_1$  not only shows regional fluctuation in the strikes, but it also shows development of a distinct crenulation. The axes of these crenulations, (viz., puckers) characterising the  $L_3$ , are very often seen superimposed over  $L_1$ . The trend of  $L_1$  also shows some effect of  $F_3$ . As  $F_1$  and  $F_3$  are to some extent co-axial, the distortion of  $L_1$  by  $F_3$  is not very conspicuous and the effect comprises a fanning of the  $L_1$  trends, such that their plunge direction fluctuates between  $N30^\circ W$  to as much as  $N25^\circ E$ .

### Effect of $F_3$ on $F_2$ —

The superimposition of  $F_3$  folds has considerably distorted the original synformal shape of the  $F_2$

structures. In the west i.e. in sub-areas (14) and (15), the north dipping limb of  $F_2$  synform has been arched-up into the Matela antiform. As a result of this, the orientation of  $L_2$  has been considerably modified. While in the sub-area (15) comprising the western limb of the  $F_3$  antiform, the  $L_2$  is seen plunging in the NW quadrant, the same plunges in the opposite direction on the eastern limb. In fact, the amount of plunge of  $L_2$  lineations in the sub-areas (6), (7), (8), (9), (10), (11) and (17) has slightly increased mainly due to the effect of  $F_3$ .

Another part of the area where  $F_3$ - $F_2$  interference is seen, is in the main hinge area (Dinapani-Kaparkhan synform) in the NE. The north dipping limb of the  $F_2$  synform is considerably distorted and is seen to form a number of  $F_3$  folds. As a result of this superimposition of folding, the  $L_2$  shows some scattering in its plunge; and the plunge direction varies from ENE to as much as SE. In the sub-area (5), where a NS trending  $F_3$  fold is encountered, the  $L_2$  shows plunge both due E and W.

#### JOINT PATTERN

The author has studied the joint pattern in a most general way, because in an area of repeated deformations,

the joints reveal very little. He has, however, recorded the most conspicuous joint sets encountered in the different parts of the area and shown them on a map (Fig.IV.25). He found that the joint system vary from one part of the area to the other. On the basis of his observations, the joint pattern of the study area could be said to comprise the following systems area wise:

Western part of the area (West of Kosi river)

The rocks of this part of the area, mainly show two prominent joint sets. One strikes almost NNE-SSW and is vertical. The other set shows low dips northward and is broadly parallel to the bedding and schistosity (the two being almost identical). Of these two sets, the latter appear to be folded on  $F_3$ , while the former (vertical joints) are either related to  $F_3$  or are even of a later origin.

Eastern and north eastern part of the area  
(East of Kosi river)

Here also the prominent joints constitute three sets, one is almost identical to the bedding joints and follows the dip and strike of the foliation. The other two are vertical and strike N-S and E-W. The N-S vertical joints which are more numerous are superimposed over the  $F_3$  folds and thus they appear to have developed after the  $F_3$  folding.

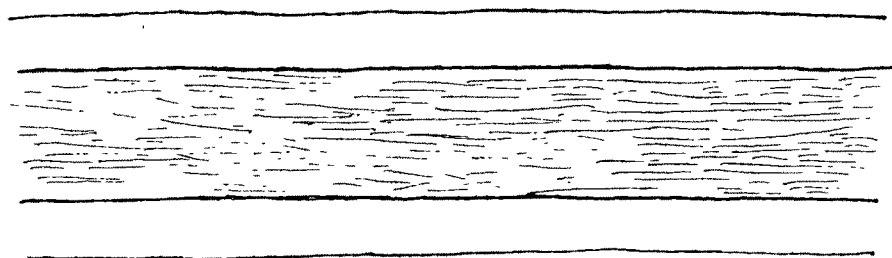
## DISCUSSION

The structural analysis and the results obtained when considered together with the outcrop pattern and foliation trends, reveal an interesting and complex structural history, comprising more than onefold episodes.

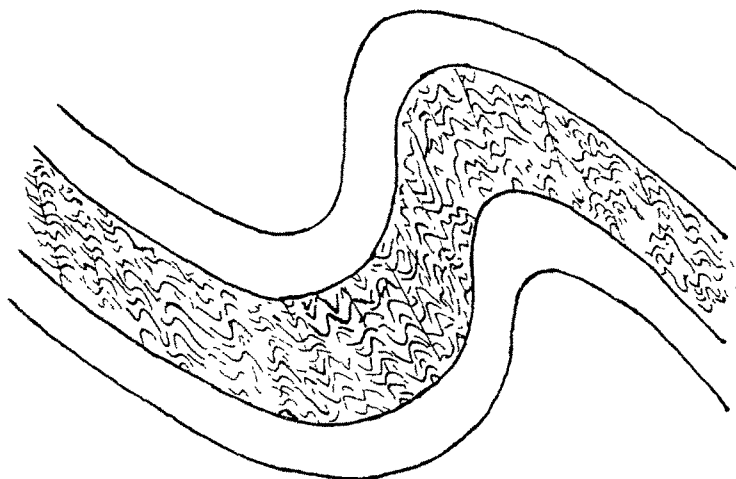
The first episode ( $F_1$ ) folded the rocks into numerous isoclinal reclined folds, whose axes at present show a northerly plunge in most of the area. The main schistosity ( $S_1$ ) of the garnet mica-schists and the graphitic schists shows axial-plane relationship with the  $F_1$  folds. This folding is the same as that referred to as recumbent folding ( $F_1$ ) by Merh and Vashi (1965) in Ranikhet area. The author has however, found that the schistosity  $S_1$ , that developed during  $F_1$  is not a direct product of the deformation and metamorphism of the unmetamorphosed sediments, but there are evidences to suggest that the  $S_1$  is derived by the microfolding of an earlier metamorphic foliation (S) and the progressive tightening of such microfolds (Fig.IV.27) finally resulting to a new cleavage ( $S_1$ ). Desai (1968,p.93) in Majkhali area has referred to S as a bedding schistosity - and he too found that, "this early schistosity in micaceous layers is almost obliterated and (on a very close scrutiny) is recorded to show its very tight microfolding and

Fig. IV . 27.

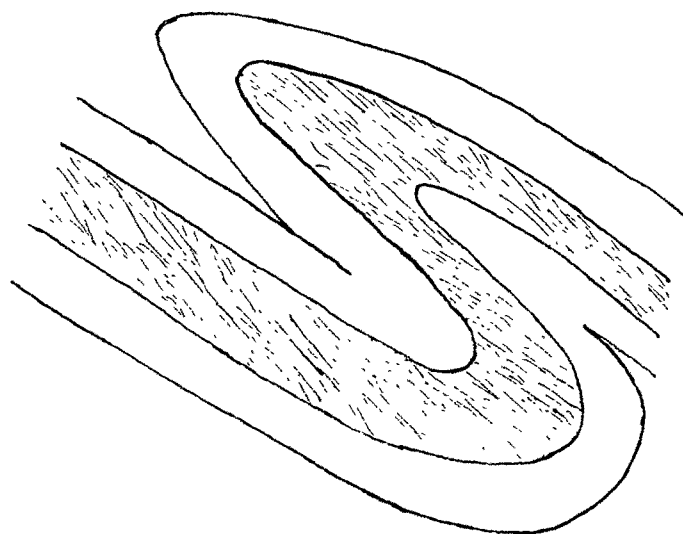
Development of  $S_1$  from  $S$ .



1



2



3

ultimately merging into  $S_1$ ." Sarkar et al. (1965) too recognised a cleavage pre-dating the main schistosity (Sarkar's  $S_2$ ), but he considered the former cleavage to be related to a set of minor recumbent folds that developed prior to the main event of isoclinal recumbent folding ( $= F_1$  of the author). The author is however very doubtful whether any such very early folding took place at all. Perhaps he mistook the  $F_1$  reclined folds showing different orientation of axes and axial planes, on account of the effect of  $F_3$ , as constituting recumbent folds of two distinct generations.

The second folding ( $F_2$ ) gave rise to the Almora nappe synform. It is clear from the related structures preserved in the study area, that in addition to the development of large macroscopic structures, this fold event is best represented by a fine crinkling of the schistosity. The axes of these microfolds and crinkles, comprise the dominant lineation related to this fold episode. It has been reported from the neighbouring areas by numerous previous workers (Merh, 1968; Vashi, 1967; Desai, 1968; Patel, 1972). Sarkar et al. (1965) do not appear to have recognised this lineation.

The superimposition of yet another fold ( $F_3$ ) on  $F_1$  and  $F_2$  structures has given rise to the existing

outcrop pattern and the foliation trend. This folding is for the most part quite open, with almost N-S axial-planes in the western part of the area, and with NE-SW axial-planes in the north-eastern corner, where the folds of  $F_3$  generation have considerably distorted the  $F_2$  synform. The swing in the trend of the  $F_3$  fold from NS to NE-SW appears to be the original property of this fold episode. It is the effect of  $F_3$  (Matela antiform) that the various macroscopic and mesoscopic  $F_1$  structures show diverse orientations. The axial-planes follow the foliation trends, with the axial plunge varies from  $N30^\circ W$  to  $N25^\circ E$ . The author suspects that this effect of  $F_3$  or  $F_1$  structures, misguided Sarkar et al. (1965) who found two generations of recumbent folds. In fact, the present study has very clearly established only one episode of isoclinal reclined folding, the flexure axes related to which show divergent orientations in different parts of the area.

The effects of  $F_3$  on  $F_2$  are not very conspicuous in the area. But when all the pucker lineations recorded in the area were plotted on the map, it was very clear that a distinct and prominent puckering is associated with  $F_3$ . It shows almost an uniform plunge in the NE quadrant. Sarkar et al. (1965) have also recorded a

similar pucker lineation and on a perusal of their map (Ibid, p.682) it is seen that though most of their  $L_4$  pucker lineations tally with the author's  $L_3$ , but some of their  $L_4$ , are in fact  $L_2$  of the author; obviously the abovesaid authors have not been able to sort out puckers related to  $F_2$  and  $F_3$ . The author does not agree with Sarkar et al. (Ibid, p.684) that the puckers represent folds subparallel to the direction of tectonic transport during the main movement of the nappe. In fact, the various lineations present in the Almora area, represent 'b' axis of successive fold episodes, the later two fold episodes having been superimposed after the nappe had formed.